CHALMERS
UNIVERSITY OF TECHNOLOGY

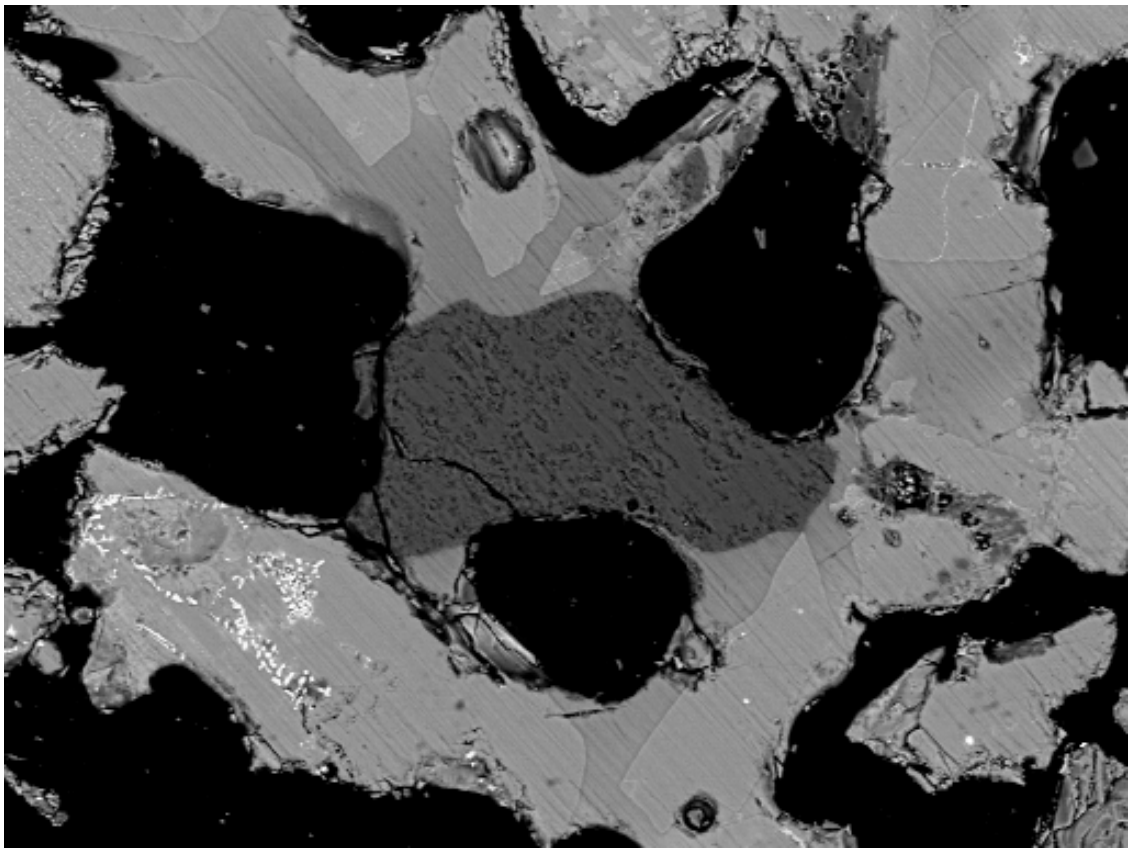

Bed agglomeration behavior in biomass firing FBC conditions

A comparison of three different bed materials

Master's thesis in Materials Chemistry

FRIDA TROPP

DEPARTMENT OF CHEMISTRY AND CHEMICAL ENGINEERING

CHALMERS UNIVERSITY OF TECHNOLOGY
Gothenburg, Sweden 2021
www.chalmers.se

Master's thesis 2021

Bed agglomeration behavior in biomass firing FBC conditions

A comparison of three different bed materials

FRIDA TROPP

CHALMERS
UNIVERSITY OF TECHNOLOGY

Department of Chemistry and Chemical Engineering
Division of Energy and Materials
Chalmers University of Technology
Gothenburg, Sweden 2021

Bed agglomeration behavior in biomass firing FBC conditions
A comparison of three different bed materials
FRIDA TROPP

Supervisor: Maria Zevenhoven, Åbo Akademi University
Supervisor: Patrik Yrjas, Åbo Akademi University
Examiner: Henrik Leion, Environmental Inorganic Chemistry

Master's Thesis 2021
Department of Chemistry and Chemical Engineering
Division of Energy and Materials
Chalmers University of Technology
SE-412 96 Gothenburg
Telephone +46 31 772 1000

Cover: Backscattered scanning electron microscopy (SEM) image of a cross-section of a agglomerate after sunflower seed shell pellets combustion, using blast furnace slag as bed material at 900°C.

Bed agglomeration behavior in biomass firing FBC conditions
A comparison of three different bed materials
FRIDA TROPP
Department of Chemistry and Chemical Engineering
Chalmers University of Technology

Abstract

When fossil fuels are phased out and replaced with biomass in energy conversion in fluidized beds, ash-related problems like fouling, sintering, and agglomeration are likely to increase. Agglomeration in a fluidized bed can cause defluidization and result in high operating costs. Biomass with high alkali content like agriculture residue and waste is especially problematic. Since the composition of the fuel is hard to change, a possible solution to the problems could be using alternative bed materials that counteract the agglomeration tendency of the biomass fuel. Therefore, this study focuses on agglomeration phenomena in fluidized beds using alternative bed materials in an attempt to avoid defluidization of the bed.

In this study, two byproducts from the steel industry, blast furnace slag, and oxide scales, were tested as bed materials in a laboratory-scale bubbling fluidized bed reactor. Both fuel and salt experiments were performed at 850°C and 900°C. Sunflower seed shell pellets were used as fuel and were fed to the reactor until defluidization occurred or until 700 g had been fed. The salt K_2CO_3, a synthetic ash component, was added to the reactor in batches of 0.5 g/10 min until defluidization occurred or until a total of 10 g had been fed. The results from the experiments with the two bed materials were also compared to previous studies performed in the same reactor using silica sand as bed material.

After each experiment, the bed was examined and analyzed with scanning electron microscope coupled with an energy dispersive X-ray analyzer (SEM-EDX). In the experiments with blast furnace slag, bed agglomerates were found to have been formed around sand particles and potassium silicate glued the particles together. In the oxide scale bed, potassium gathered around the particles, and only very small amounts of potassium silicate could be found after combustion with sunflower seed shell pellets.

Both blast furnace slag and oxide scales proved to be able to withstand higher weight percentages of potassium in the bed before defluidization occurred compared to silica sand. This indicates that they could be more suitable bed materials than silica sand for fuels with a high potassium content such as sunflower seed shell pellets.

Keywords: bubbling fluidized bed combustion, silica sand, blast furnace slag, oxide scale, sunflower seed shell pellets, potassium carbonate.

Acknowledgements

I would like to thank my examiner Henrik Leion and my supervisors Maria Zevenhoven and Patrik Yrjas for the opportunity to perform my master thesis at Åbo Akademi University in Åbo/Turku, Finland despite the COVID-19 pandemic.

I also want to thank Christoffer Sevonius, Peter Backman, Linus Silvander, Tor Laurén and Jaana Paananen for the help and consultation during the practical part of the project and for always taking time for my questions.

Furthermore, I would like to thank Erasmus+ for financial support during my time in Finland.

Last but not least, I would like to thank my partner Christian Persson for his support.

Frida Tropp, Gothenburg, June 2021

Contents

List of Figures

List of Tables

1
Introduction

Fossil fuels are being phased out in the energy and heat sector and are replaced by biomass fuels. Biomass fuels can in some cases be a bit more problematic during combustion due to their different ash composition. The fluidized bed combustion technique has a high fuel flexibility which makes it suitable for biomass combustion [1]. High fuel flexibility means that it can handle a lot of different fuels and fuel qualities [2].

The fluidized bed technology is based on the use of a bed material that is fluidized in the boiler. Fluidization occurs when an air stream passing through a bed of particles is strong enough to make the bed behave like a liquid [2]. The bed material distributes heat in the bed resulting in a more even temperature both in different parts of the reactor, but also over time. This aids the combustion and makes it more efficient [1].

Biomass, especially waste products and residues from for example agriculture, contains high amounts of alkali compounds. The high alkali content is known to cause problems with fouling, corrosion, and agglomeration [3]. When the mean size of the bed particles increases as a result of the agglomeration the airflow will eventually not be able to fluidize the bed and the bed will defluidize. Defluidization results in unscheduled shutdowns which is costly for the industry [2].

The combustion of biomass is considered to be nearly CO_2-neutral and can in combination with carbon capture even result in negative CO_2 emissions. It is therefore important for the environmental impact of the process to use biomass instead of fossil fuels [4]. Several different methods can be used to minimize or prevent the problems associated with biomass combustion. For example, pre-processing, co-combustion of fuels, and the use of alternative bed materials [5]. Changing the composition of the bed material will affect the interactions between the bed material and the fuel. Finding suitable fuel and bed material combinations could therefore counteract the problems associated with biomass combustion, even for more problematic fuels.

The research of bed materials for fluidized bed combustion could also benefit other techniques using fluidized bed technology. One example is oxygen carrier aided combustion (OCAC), which uses a bed material that can transport oxygen in the bed. For example, iron oxide-containing materials can both oxidize and be reduced in the boiler making it possible to transport oxygen from oxygen-rich parts to oxygen-lean parts of the boiler, aiding the combustion [6].

Another technique using oxygen carriers is chemical looping combustion (CLC). This technique uses two different fluidized bed reactors and the bed material is circulated between the beds. The bed material is first oxidized by air in the air

reactor and then the combustion takes place in the fuel reactor using the oxygen that the bed carried from the air reactor. Since the fuel and air are kept separate it is possible to get the exhaust gas from the fuel reactor to consist mainly of CO_2 and H_2O. The water can be condensed leaving a nearly pure CO_2 stream, which makes CLC very suitable for carbon capture methods since no gas separation is necessary [7].

Today the most commonly used bed material is silica sand [1] but the search is ongoing for materials that can counteract agglomeration of certain fuels, aid the combustion, and is still cheap enough.

1.1 Aim

During this project two different waste materials from the steel industry, blast furnace slag and oxide scales, were used as bed materials in a laboratory-scale bubbling fluidized bed reactor. The aim of this study was to examine how the two bed materials interact with the ashes from sunflower seed shell pellets. K_2CO_3 was also used as a synthetic ash component to further examine the interactions between the bed materials and potassium. The goal was to compare the two tested materials and previous results from similar experiments using silica sand as bed material.

1.2 Specification of the issue under investigation

To specify the aim further, this section divides the aim of the project into several questions that should be answered during the project. The questions are the following:

- Is there a difference in how the bed materials interact with the fuel?
- What could be the reason for this difference?
- How does the temperature affect the outcome of the experiments?
- For every experiment:
  - Did the bed defluidize and if so, after how long time and/or after how much fuel/salt was fed?
  - Was it possible to find agglomerates in the bed after the experiment?
  - What elements seem to play a major role in causing the defluidization and/or agglomeration and how much of the element(s) the bed can withstand before defluidization?

1.3 Limitations

Due to the time available, the project was limited to an experimental matrix containing two bed materials (blast furnace slag and oxide scales), two temperatures (850 °C and 900°C), one fuel (sunflower seed shell pellets), and one salt (K_2CO_3).

Another way that time affected the project was that the length of the experiments needed to be adapted to the length of a workday. Therefore all experiments had to have a maximum amount of fuel or salt that was to be added to the reactor if no defluidization occurs before that.

2

Theory

This chapter will introduce concepts, techniques and materials important for this project. This includes the three bed materials silica sand, blast furnace slag, and oxide scale, which will be compared.

2.1 Fluidized bed boiler

Fluidized bed combustion (FBC) is a technique where a bed material is used in the combustion unit. An airflow from the bottom of the reactor fluidizes the bed material, making the bed behave like a fluid rather than solid particles [2]. The main function of the bed material is to transport heat, which evens out the temperature both in different parts of the bed and over time. The bed material can also affect emissions, corrosion, and agglomeration depending on interactions between the bed material and the ashes formed during the combustion [1].

There are two main versions of fluidized beds, bubbling fluidized beds (BFB) and circulating fluidized beds (CFB). As the name might suggest the bed material in a BFB is bubbling and behaves like a boiling liquid. A CFB consists of two parts, a boiler and a cyclone. This technique uses a higher airflow which makes part of the bed particles exit through the top of the reactor, where they are gathered in a cyclone and returned to the bed at the bottom of the boiler. The circulation of the bed material requires smaller bed particles (0-25 mm compared to 0-50 mm for BFB) and a higher airflow (fluidization velocity of 3-10 m/s compared to 1-3 m/s for BFB) [2].

Fluidized bed combustion is suitable for solid fuel combustion [1] and has high fuel flexibility, which means that it can handle a lot of different fuels and fuel qualities [2]. For example, different biomass materials and waste streams. The BFB can handle lower quality and higher moisture content than CFB, resulting in that BFB often operates at slightly lower temperatures than CFB [2].

The use of fuels like biomass and waste is likely to increase the agglomeration problems in the boiler. This is usually prevented by continuous regeneration of the bed material [8]. During biomass combustion, a third of the bed may need to be replaced each day, and for waste incineration as much as the entire bed may need replacing. A general rule for regeneration of bed material is 3 kg/MWhth during biomass combustion and 6 kg/MWhth during waste incineration. This makes the material cost an important factor in the choice of bed material. Today the most commonly used bed material is silica sand [1].

2.2 Biomass fuels

In the context of biomass combustion, one normally only refers to plant-based material as biomass [5]. The combustion of biomass is considered to be nearly CO_2-neutral and can in combination with carbon capture and storage, so called bio-energy with carbon capture and storage (BECCS), have negative CO_2 emissions. There is an ongoing transition in heat and power production to use biomass instead of fossil fuels like coal and oil. Fluidized bed combustion is often used for biomass combustion due to its flexibility and good heat transfer [4], but the use of biomass also comes with some challenges. For example, biomass combustion usually has more problems with corrosion, fouling, and agglomeration than fossil fuel combustion [5].

2.2.1 Biomass ashes

Different kinds of biomass usually have quite similar carbon, oxygen, and hydrogen content [5], but the composition of the ash forming matter have large variations [9]. The composition of the ash forming matter depends on the kind of biomass. For example, wood and forest residues usually mainly contains Ca, K, and P. The fuel is often also contaminated with sand, which contributes with Si and Al. Agriculture residues can also be used as fuel and this group has an even larger variation of the composition. The main ash forming matter components are usually Si, K, Ca, P, and Cl, but for example straw have high concentrations of K, Cl, P, and S. Still, the composition varies between different fuels and therefore every fuel needs to be analyzed to know the ash forming matter composition [9].

The ash forming matter composition has a huge impact on what problems will occur, but there are still no certain ways to predict how a new fuel will behave. There are many methods that can give indications of the ash behavior, but it is still just predictions. The following section will describe some known ash reactions.

2.2.2 Ash components

K is present in biomass as a salt or organically bound ions, that are released and forms KOH(g), K(g), and KCl(g) during combustion. The proportions between the compounds will depend on what other compounds are present. For example, if there is no Cl present the main gases will be K(g) or K_2CO_3(g) under reducing conditions and KOH(g) under more oxidizing conditions. If Cl is present the main vapor will be KCl(g) [9].

The availability of S will affect the further reactions of the K-containing gases. S can be found in biomass as SO_4^{-2} or organically bound S, and most of it will form SO_2 during combustion. When there is no S available K(g) and KOH(g) will react according to Equation 2.1. The carbonate particles formed this way are aerosols, which melt at around 890°C [9].

$$2KOH(g) + CO_2(g) \leftrightarrow K_2CO_3(s,l) + H_2O(g) \tag{2.1}$$

In the absence of S, KCl(g) will condense on existing fly ash or as aerosols. KCl has a melting point of 770°C, it is highly corrosive and tends to make the ash stickier

at lower temperatures. It is also known to cause high-temperature corrosion if it gets in contact with the boiler walls [9].

The presence of S will change how the K-containing compounds react. KCl and KOH will react with SO_3 and form $KHSO_4$ and KSO_3Cl respectively, which will then react according to Equation 2.2 and 2.3 to form K_2SO_4 [9].

$$KSO_3Cl(g) + H_2O(g) \leftrightarrow KHSO_4(g) + HCl(g) \tag{2.2}$$

$$KHSO_4(g) + KCl(g) \leftrightarrow K_2SO_4(g) + HCl(g) \tag{2.3}$$

Those reactions will decrease the amount of Cl in the fly ashes, which will decrease the corrosion on the superheaters. Several techniques are using this reaction by adding sulfur to the boiler. Na usually reacts very similarly to K but with less impact since the Na concentration in the fuel usually is much lower [9].

K also affects the behavior of Si. Si usually forms high melting ash, which is relatively inert during FBC conditions. However, there are some exceptions. For example, some agriculture residues like straw, which contain equally high concentrations of K and Si, will form low-melting potassium silicates. Those low melting compounds will result in major fouling and sintering problems in the boiler. Both Si and Al, which are usually not very reactive, can indirectly affect fouling and corrosion problems by affecting the chemistry of compounds like K, Na, and Ca in the boiler [9].

Ca in the form of silicates is not reactive, but when it exists as CaC_2O_4 or organically bound in the biomass it will form CaO during combustion. The CaO then forms aerosols which will participate in further reactions in the flue gas. It can for example bind S during a sulfination reaction, see Equation 2.4 [9].

$$CaO(s) + SO_2(g) + \frac{1}{2}O_2(g) \leftrightarrow CaSO_4(s) \tag{2.4}$$

This reaction can reduce the SO_2 content in the flue gases and sometimes limestone is added to the process to get this effect. The use of limestone will result in bigger CaO particles than the ones formed from the Ca in the fuel and therefore be less reactive, due to the lower surface area. A high CaO concentration can capture almost all S, making the sulfation of alkali chlorides decrease significantly. CaO can also undergo recarbonation, see Equation 2.5, which can cause fouling. This reaction occurs between 600°C and 800°C [9].

$$CaO(s) + CO_2(g) \leftrightarrow CaCO_3(s) \tag{2.5}$$

Mg reacts in the same way as Ca, but at lower temperatures which makes it less relevant in FBC conditions [9].

P can form both calcium and alkali phosphates during combustion. Calcium phosphates usually do not cause any problems but alkaline phosphates does often have low melting points which can cause both bed sintering and deposit formations. The Ca/K ratio in the fuel can indicate if alkali phosphate-related problems will occur during the combustion [9].

2.3 Agglomeration

There are two kinds of interactions in a fluidized bed, gas-particle and particle-particle interactions. Early research focused mainly on the gas-solid system, which resulted in the Erguan equation. The Erguan equation can be used to calculate the gas velocity needed to fluidize a bed. Later other models were developed to also account for the interactions between the particles. Small particles are for example affected by electrostatic forces and van der Waals forces. The presence of a liquid phase on the particle will also affect the interaction between particles. If the inter-particle forces become larger than the forces from the fluidization gas the particles will agglomerate and the gas flow pattern will change. Eventually channels will occur in the bed and the bed will defluidize [10].

Agglomeration and defluidization in fluidized bed combustion is usually caused by low-melting ash. The formation of alkali silicates is common and they often have lower melting points than the individual components. For example, potassium silicate has a eutectic temperature below 770°C which is lower than the typical operating temperature during fluidized bed combustion (800-850°C) [10].

Agglomeration results in a wider size range of the particle distribution, which causes segregation in the bed where larger particles gather at the bottom of the bed. This effects the mixing of the bed material, fuel and fluidization gas, resulting in an uneven temperature distribution and eventually defluidization of the bed. The agglomeration process is often not detected until defluidization occur. In industrial scale defluidization of the bed is costly since it results in lengthy unscheduled shutdowns of the process [10].

The most commonly used bed material in fluidized bed combustion is silica sand. Silica sand is known to agglomerate when exposed to alkali compounds, especially K. Several different mechanisms have been proposed for the agglomeration of silica sand, including the following examples [10].

- One proposed mechanism consists of three separate steps. First, ash is deposited on the bed particle surface by attachment of small particles or condensation of gases. Then the layer buildup continues while the inner layer is homogenized and finally agglomeration occurs [10].

- Another explanation is that the agglomerates are formed around the fuel particles. The heat from the combustion causes inorganic compounds to emerge at the surface of the particle, making it sticky. When sand particles collide with the sticky particle they get stuck on the surface. The sticky melt spread on the sand particles resulting in agglomeration [10].

- A third alternative is that there are two kinds of agglomeration, melt-induced and coating-induced. Melt-induced agglomeration occurs when melted ash particles end up between colliding sand particles and glue them together, while in coating-induced agglomeration a uniform layer is built up around the particle. The layer can then cause agglomeration when particles collide [10].

To avoid unscheduled shutdowns of the process due to defluidization it is important to detect agglomeration early. Several different methods have been proposed for detection of agglomeration, both off-line and on-line methods. Off-line methods are methods analysing the fuel and/or bed material outside the fluidized bed. This kind of methods can give directions in well-known cases with small fuel variations. When the measurement is performed in the reactor it is called on-line and there are several examples of on-line methods, such as pressure, acoustic, and temperature measurements [10].

Pressure measurements reflect the hydrodynamics of the fluidized bed and can be used for both linear and non-linear methods. Linear methods are also sensitive to other fluctuations in the bed and for example changes in superficial gas velocity can cause false alarms. It is therefore not suitable as agglomeration indicator in industrial applications. Principal component analysis (PCA) has been tested to increase the reliability, but requires further testing. The reliabillity of non-linear methods are still unclear. Kullback–Leibler distance and the W-statistic method have proven to be sensitive for agglomeration, but it is still uncertain how they react on other process changes [10].

Temperature measurements can be used to indicate agglomeration, but since it experiences slower dynamics than pressure the indication will come at a later stage of the agglomeration process. Acoustic measurements have been used to indicate other changes in the bed. Therefore it might be possible to use acoustic measurements to discover agglomeration in the bed, but it needs to be tested for this use case [10].

When agglomeration has been detected in the bed there are some alternatives that can be used to avoid defluidization. In industry it is common to reduce the fuel feeding rate, change ratio between two co-fed fuels in favor of the safer alternative, or entirely switch fuel. Another option is to lower the temperature and increase the gas flow, but that is to be considered a emergency measure since it has a drastic negative impact on the operation [10].

There are also many preventive ways to counteract agglomeration in fluidized bed combustion. For example, using additives, alternative bed materials, or manipulating operating conditions. Several different additives have been tested in fluidized bed combustion. The main idea with additive addition is to make the alkali components from the fuel react with the additive and form compounds with higher melting points than the combustion temperature [10].

Another alternative is to minimize the silica content in the reactor by using alternative bed materials. Alternative bed materials often consists of Al, Mg, Ca, Fe or any mixture of them. There are still fuels like straw which contains both high amounts of Si and K, where avoiding Si in the bed material will not be enough to prevent potassium silicate-induced agglomeration. Alternative bed materials usually delay defluidization rather than eliminate it. During both additive addition and the use of alternative bed materials several aspects affect the usage, such as cost and treatment of the bed material after use [10].

There are also several patents on reactor designs meant to remove agglomerates during the operation of the boiler and other design ideas. Evaluations of this kind of methods are rarely published and its efficiency is therefore uncertain [10].

2.4 Bed materials

There are many different materials that can be used as bed materials and the following sections will present five of them, including silica sand, blast furnace slag, oxide scale, LD-slag and ilmenite. Bed materials can be divided into two groups, active and non-active materials, depending on weather they can transport oxygen or not. Active bed materials, also called oxygen carriers, are materials which can transport oxygen.

2.4.1 Non-active bed materials

Non-active bed materials do not posses the ability to transport oxygen. Silica sand and blast furnace slag are two examples of non-active bed materials.

2.4.1.1 Silica sand

Quartz is the second most abundant mineral [11] and makes up around 26 wt% of the earth's crust [12]. Quartz sand, also known as silica sand, consists of SiO_2 [11]. It can be used for many different applications, for example, to manufacture glass and ceramics, or used in sandpaper [11], portland cement, concrete, and mortar [13]. Silica sand is the most commonly used material in commercial fluidized bed boilers [1].

One study, examining the layer build-up on the silica sand bed particles during fluidized bed combustion, concluded that two layers usually form on the particle [14]. The inner layer consists mostly of Ca, K, Si, and O, while the composition of the outer layer more closely resembles the composition of the fuel ash [14].

The interaction between silica sand and K_2CO_3 was also examined in a study [15]. Using thermogravimetric analysis (TGA) measurements it was found that the pure K_2CO_3 starts to decompose at around 1150°C, while a mixture of silica sand and K_2CO_3 experience a significant mass loss between 700°C and 1100°C. This indicates that the mass loss is caused by a reaction between the silica sand and K_2CO_3. Thermodynamic calculations also indicated that the formation of potassium silicates are favourable above 600°C [15].

The same study also examined how different conditions affected the reaction rate and the conversion of K_2CO_3 in a silica sand bed. It was found that the conversion rate increased with the temperature (700-850°C). Complete conversion was observed from 750°C, but at 700°C only a conversion of 0.8 was observed. This is explained by the fact that a molten phase is possible above 750°C which would improve the conversion [15].

They also examined the impact of particle size for the K_2CO_3 by using two different sizes at two different temperatures (750 and 800°C). The smaller size resulted in both higher reaction rate and conversion. They also found that the partial CO_2 pressure affected both the conversion and the reaction rate. The presence of CO_2 (50% and 100%) proved to decrease both reaction rate and conversion, but the difference between 50% and 100% CO_2 was insignificant [15].

When three different molar ratios (SiO_2:K_2CO_3 45, 77 and 111) were tested no significant differences were observed. The mixing of the K_2CO_3 turned out to be

important for both conversion and reaction rate. Again three different setups were used. The first was well mixed, the second was a even layer of K_2CO_3 on top of the silica sand and the third one a localized layer on top of the silica sand. The well-mixed setup proved to be most effective and resulted in the highest reaction rate. It was followed by the even layer, and after 4 h both the well-mixed and the even layer experiment had reached almost complete conversion. The localized layer on the other hand experienced both the lowest reaction rate and lowest total conversion [15].

In another study, the interactions between several different potassium salts and silica sand were examined using a laboratory-scale BFB reactor [16]. KCl, K_2CO_3 and K_2SO_4 were used as synthetic ash components to enable the examination of the interaction of specific parts of the ash with the bed material. Four different temperatures (750, 800, 850, and 900°C) were used and the experiments were performed both in dry and wet conditions. KCl evaporates at the temperatures used in the reactor, resulting in higher amounts of salt needed to cause defluidization at higher temperature. No reaction with the bed material was found and instead, pure KCl was found gluing the particles together. The presence of water decreased the evaporation of the salt, resulting in that lower amounts of salt was needed to cause defluidization [16].

K_2CO_3 was the only salt in the study which caused similar agglomerates as the ones found in full-scale boilers. The amount needed for defluidization decreased with increasing temperature and wet conditions had little effect on the results. All K_2CO_3 were assumed to stay in the bed during the experiments. K_2SO_4 did not cause any defluidization and stayed inert during the experiments. Unreacted K_2SO_4 particles were found in the bed [16].

2.4.1.2 Blast furnace slag

Blast furnace slag is a byproduct from the process where iron ore is converted into pig iron in a blast furnace [17]. The main components are silica oxide, calcium oxide, magnesium oxide, and aluminum oxide, but it also contains smaller amounts of several other oxides [14]. Blast furnace slag can be used as construction material and for building roads [18].

Blast furnace slag has for example been compared with silica sand as a bed material using several different fuels. During combustion of bark and olive residue, the blast furnace slag had a between 25 and 60°C higher initial agglomeration temperature. When canary grass was combusted at 800°C it took 380 min before agglomeration was detected compared to 280 min for silica sand. The study also tested straw and peat, where straw quickly caused agglomeration of both bed materials and peat did not show agglomeration during the performed experiments [14].

The layer build-up around the particles was also studied. Blast furnace slag showed much thinner layers than the silica sand and the inner layer was only present in some of the samples. The outer layer was porous and inhomogeneous, with a composition similar to the one of the fuel ash. When two layers could be identified the inner layer was enriched in Ca and contained lower amounts of some of the fuel ash components. For the blast furnace slag, the molten outer layer was the cause of agglomeration. Chemical equilibrium calculations were used to explain the

lower agglomeration tendency of the blast furnace slag compared to the silica sand. The composition of the blast furnace slag turned out to be close to the calculated equilibrium, which would explain the lower reactivity with K and Ca [14].

Another study examined different solutions to the agglomeration problems caused by straw and other problematic fuels in a silica sand bed. One of the examined methods was to use blast furnace slag as bed material instead of silica sand. The experiments were carried out in a 12 MW circulating fluidized bed and the use of blast furnace slag as bed material was found to counteract bed agglomeration [19].

2.4.2 Active bed materials

Active bed materials, also called oxygen carriers, are transient matierals, often metal oxides which can have different oxidation states [6]. This makes it possible for the material to transport oxygen in the bed. A more even oxygen distribution aids the combustion and makes it more efficient [20].

Many criteria need to be fulfilled for a material to be considered a good oxygen carrier [20]. The material needs to have a high enough reactivity towards both oxygen and the fuel. It also needs physical properties like mechanical strength and a high enough melting point, to avoid problems with sintering and attrition in the boiler [21]. The fluidizing properties are important and a good oxygen carrier should have stable reactivity, since an increasing reactivity often is associated with an increasing porosity, which can cause fragmentation [22]. It is also important to consider the environmental impact of the oxygen carrier both before, during, and after use in the boiler [21].

Initially, the research on oxygen carriers was mostly focused on synthetically made materials, but the problems associated with the combustion of solid fuels changed that [22]. The high regeneration rates associated with many solid fuels made material cost an important factor to consider for a potential oxygen carrier [21]. The focus has therefore changed from synthetically produced oxygen carriers to low-cost materials such as naturally occurring minerals and byproducts, which is the main focus of the research today [22].

Many materials could potentially be used as oxygen carriers. Different oxygen carriers react differently with ash components, which will make them work better with different fuels [23]. This section will present some techniques using oxygen carriers and three active bed materials (oxide scale, LD-slag and ilmenite).

2.4.2.1 Oxygen carrier-aided techniques

There are several techniques based on the use of oxygen carriers, for example oxygen carrier aided combustion, chemical looping combustion and chemical looping gasification which are presented in this section.

2.4.2.1.1 Oxygen carrier aided combustion Oxygen carrier aided combustion (OCAC) is a technique where the bed in a fluidized bed boiler is partially or fully replaced with an oxygen carrier [20]. The oxygen carrier, often a metal oxide, can undergo both reduction and oxidation under the conditions in the boiler.

The material is oxidized by the combustion air in oxygen-rich parts of the reactor, according to reaction 2.6. Oxidized oxygen carriers can then react with volatile compounds in oxygen-lean parts of the boiler, forming water and CO_2, see reaction 2.7 [6].

$$x\mathrm{M(s)} + 0,5\mathrm{O_2(g)} \rightarrow x\mathrm{MO(s)} \tag{2.6}$$

$$n\mathrm{C_iH_j(g)} + x\mathrm{MO(s)} \rightarrow x\mathrm{M(s)} + y\mathrm{CO_2(g)} + z\mathrm{H_2O(g)} \tag{2.7}$$

where M is the reduced oxygen carrier and MO the oxidized version.

OCAC is a way to improve the oxygen distribution in the boiler that can enable a lower amount of excess air to be used without increasing the emissions. The improved distribution of oxygen can minimize the formation of reducing zones in the bed. Oxygen carriers can also work as an oxygen buffer in case of load changes or uneven fuel addition [1]. Some oxygen carriers might even have a positive effect on some of the problems associated with biomass combustion, such as sintering, agglomeration, fouling, and corrosion issues [5]. The OCAC concept enables new boiler designs. For example, the change in the temperature profile caused by the improved combustion in the bottom of the bed could make it possible to decrease the height of boilers. Although the biggest advantage with the OCAC technique is probably that it can be implemented in already existing FB boilers to improve their efficiency [20].

2.4.2.1.2 Chemical looping combustion Chemical looping combustion (CLC) is a technique using two fluidized bed reactors. One (the air reactor) for oxidizing the oxygen carrier bed material and one (the fuel reactor) for combustion of the fuel. The bed material is reduced in the fuel reactor and the oxygen is used for the fuel combustion. By using two reactors the air and the fuel are separated from each other, which is called unmixed combustion. This has an important effect on the exhaust gases from the process since the air reactor emits air and hydrogen gas and the fuel reactor can be operated to generate a CO_2 and H_2O stream. The CO_2 gas can then be separated by condensing the water, which makes CLC a very suitable technique for carbon capture methods since no gas separation is required [7].

2.4.2.1.3 Chemical looping gasification Chemical looping gasification (CLG) is similar to CLC in the sense that it also consists of two separate fluidized beds, called gasifier and regenerator. During gasification, the fuel is not entirely oxidized like in CLC but is instead transformed into syngas. Gasification typically occurs between 800°C and 900°C and can be used to produce hydrogen gas [24].

CaO can be used in CLG to transport both oxygen and CO_2. The fuel is gasified in the gasifier in the presence of CaO and steam, producing a hydrogen-rich stream. During the gasification, the produced CO_2 directly reacts with the CaO forming $CaCO_3$. The $CaCO_3$ is then circulated back to the regenerator where it is calcined resulting in a highly concentrated CO_2 stream and the regenerated CaO can be reused in the gasifier [24].

2.4.2.2 Oxide scales

When hot steel is exposed to air, an iron oxide film is formed on the surface. The film flakes off during the steel rolling process and the byproduct is called oxide scales, iron oxide scales, or mill scale [25]. The composition of oxide scales depends both on what process and what steel is used and the Fe content is usually about 70 wt%. Between 20 and 50 kg oxide scales are produced per ton of steel product, but its composition makes it possible to reuse about 90% of the material in earlier steps in the steel production [26]. Oxide scales are contaminated with oil and grease from the rolling process. The fractions with less oil contamination can be reused in earlier steps in the process, resulting in a waste with higher oil content. Therefore oxide scales need to be heat treated to remove the oil if it is to be used as an oxygen carrier. The heat treatment can cause some agglomeration, which can make it necessary to grind and sieve the particles to get a suitable size range [27].

Oxide scales have been examined under lab-scale CLC conditions [22, 27–29], where it has showed high reactivity towards syngas, methane [22], and solid fuels [29]. The conversion of H_2 and CO is higher for oxide scale samples than for ilmenite [28]. Overall most results seem promising and the material fulfills nearly all requirements set in the studies, except that the reactivity is not stable and instead increases over time [22, 29]. In another study, the experiments with oxide scales had to be ended after 37 h in a CLC boiler due to agglomeration problems, while ilmenite was still working after 85 h [27]. The agglomeration problems were probably caused by the oxide scale particles being reduced too far due to too long residence time in the fuel reactor. Oxide scales also showed a higher attrition rate and requiring addition of more new material to the reactor compared to ilmenite [27].

The interactions between oxide scales and synthetic ash components have also been tested [30]. The tests were performed in a fixed-bed reactor at 850°C and using TGA. The salts used in the study were KCl, K_2CO_3, K_2SO_4 and KH_2PO_4. For KCl the oxide scale surface showed fragmentation and no K could be found in the bed after the experiment. The reduction rate increased when K_2CO_3 was used, but the fragmentation of the particles increased and only small amounts of K were found in the bed afterward. Low amounts of K were also found after the K_2SO_4 experiments and the SEM-EDX analysis indicated some diffusion of K into the oxide scale particle. The surface and the reduction rate of the bed material were not affected by the K_2SO_4 experiments. The only salt in the study that caused agglomeration was KH_2PO_4, which formed a low-melting K-P-Fe compound that resulted in bridge formations between the bed particles. This also decreased the reduction rate of the oxide scales. The study showed that oxide scales have a lower ability to capture the potassium salts compared to ilmenite [30].

2.4.2.3 LD-slag

Linz-Donawitz (LD) slag is a byproduct from the basic oxygen-blown converter process, also called the Linz-Donawitz process, during which pig iron is converted into steel [1]. Ca and Fe are the main compounds in the slag, but it also contains some Si, Mg, Mn, and V. LD-slag is a heterogeneous material that usually contains four different phases. One phase consists mainly of Fe, Mg, Mn and some V, in the

form of oxides. This phase does not contain any Ca and has a magnetite structure. Another phase which is usually located in small bubbles inside the slag particles consists mainly of magnesium oxide. There is a Ca phase that contains some Si and transition metals and one phase consists of Si and Al [21].

The composition of the slag depends on the origin of the iron ore used for the production [18]. Since the slag has a high calcium content, some of it can be reused replacing part of the limestone in the blast furnace. The blast furnace is the first step in the steel production, where pig iron is produced from iron ore. Only a fraction of the LD-slag can be reused in the blast furnace, for example in Sweden only around half of the more than 300 kton of LD-slag produced every year can be reused that way. This makes LD-slag the second most abundant byproduct from steel production. The demand for the remaining material is low. Some is used as construction material and some efforts have been made to use it for producing V [1]. The Fe content of about 17 wt% makes LD-slag a potential oxygen carrier [21], which has resulted in several studies of the material.

LD-slag has for example been tested as bed material in a 12 MWth circulating fluidized bed boiler fueled by wood chips. The operation worked well and without agglomeration issues, but too high CO emissions were obtained. This is thought to be caused by the LD-slag's low affinity for absorbing ash components like K. That would result in increased amounts of K in the reactor and since alkaline metals are known to be possible inhibitors of the oxidation of CO in the temperature interval of the process, that could cause the increase in CO emissions. The study also tested different methods for reducing the CO emissions, for example mixing the bed material with 50%, 70%, and 90% silica sand proved to successfully reduce the CO emissions. When LD-slag is compared to ilmenite and manganese ore, they all have slightly higher NO emissions than sand, but ilmenite and manganese ore does not increase the CO emissions as LD-slag does [1].

The amount of fly ash obtained also increased about three times during the study, compared to when using sand. This is thought to be caused by the big fraction of small particles (10-15 wt% was below 90µm) in the bed material, which leaves the boiler with the airflow. That part of the fly ash originated from the bed material was also indicated by the V content in the fly ash since V is only present in the bed material and not in the fuel [1]. During the study, bed samples were also taken to examine how the particles reactivity towards the fuel was affected by the residence time in the 12 MWth boiler. Bed samples from the boiler were tested under CLC conditions in a lab-scale FB with syngas, methane, and C_6H_6 as fuels. The reactivity towards the fuels proved to be slightly reduced by the time in the boiler, probably due to interactions and accumulation of alkaline compounds from the fuel ash [21].

LD-slag's interaction with potassium salts has also been investigated [30]. The study used synthetic ash components KCl, K_2CO_3, K_2SO_4, and KH_2PO_4 in a lab-scale fixed-bed reactor at 850 °C. The bed material and salt mixture were reduced for 6 h in CO and steam. This study showed that LD-slag has a lower ability compared to ilmenite to capture the studied salts. KCl did evaporate and no K was found in the bed after the experiment. When KH_2PO_4 was used, K-P-Ca components with high melting points formed and caused agglomeration, but without affecting the reduction rate. Both K_2CO_3 and K_2SO_4 resulted in K enrichment in the bed

and the distribution of K and V closely resembled each other. V also migrated to the particle surface during the K_2CO_3 experiment but at the same time the K_2CO_3 inhibited the reactivity. In this study only KH_2PO_4 caused agglomeration [30].

2.4.2.4 Ilmenite

Ilmenite (FeTiO3) is an iron and titanium mineral and the most abundant titanium mineral on earth [31]. It is a naturally occurring mineral and has for example been used to replace part of the bed material in the 12 MWth circulating fluidized bed boiler at Chalmers. The sand bed was continuously replaced with ilmenite over two days increasing the amount of ilmenite to 40 wt% (800 kg ilmenite in the 2000 kg bed) and then the amount was kept constant for the two remaining days of the experiment. Wood chips were used as fuel during the entire experiment. During the time in the reactor, the Fe migrates to the surface of the particle, where it forms a layer and the Ti stays in the particle core. Two additional layers are also formed due to ash compounds reacting with the ilmenite. The inner of the layers (formed outside the iron layer) is homogeneous, with a constant thickness, and is thought to be caused by a reaction between the ash components and the bed particle. The outer layer is inhomogeneous with a varying thickness and a composition similar to the fly ash. This layer was thought to grow outwards and to be caused by the ash sticking to the particle without any reaction [32].

During the same experiment, the K was also found to diffuse into the particle, where it after 24 h could be found to form KTi_8O_{16}. This will reduce the amount of K in the boiler, probably reducing both corrosion and agglomeration issues. In an attempt to see if the ilmenite could be regenerated, leaching of the used particles was performed with the goal to remove K. The particles were leached in deionized water for 72 h but only 0.2 wt% Ca and 1 wt% K were dissolved [32].

Ilmenite has also been examined for use in CLC applications, for example in one study examining its reactivity towards syngas and CH_4. During three days of experiments including around 37 reductive and oxidative cycles the reactivity with the two fuels was tested. The ilmenite was found to give a moderate conversion of CH_4 but a high conversion of syngas. Defluidization only occurred when the material was highly reduced and no decrease in reactivity was found over the three days of experiments [31].

The interactions between ilmenite and synthetic ash components in the form of potassium salts have also been examined. In one study the ilmenite was heat-treated for 6 h at 950°C before it was exposed to the four different potassium salts K_2CO_3, K_2SO_4, KCl, and KH_2PO_4. The amount of salt used for the experiments was calculated to result in 4 wt% K in the bed. The experiments were performed in a fixed-bed in a tube furnace and with TGA in both dry and wet conditions (except that KCl was not used in the TGA to avoid corrosion) [33].

During the experiments, KCl evaporated only leaving small amounts of K in the bed. The oxidation and reduction time for ilmenite decreased during the experiments with K_2CO_3 and K_2SO_4, and the amount of K absorbed by the material was significant. KH_2PO_4 was the only salt found to increase the amounts of agglomerates found. The formed KPO_3 caused a layer around the particle hindering the oxygen transport [33].

3

Method

During the project, blast furnace slag and oxide scale was used as bed materials. The interactions between the two bed materials and sunflower seed shell pellets as well as the salt K_2CO_3 were examined at two different temperatures. The experimental matrix can be seen in Table 3.1.

Bed	Fuel/salt	Temp (°C)
Blast furnace slag	Sunflower seed shell pellets	900
		850
	K_2CO_3	900
		850
Oxide Scale	Sunflower seed shell pellets	900
		850
	K_2CO_3	900
		850

Table 3.1: Experimental matrix for this study.

The following sections contain a description of the experimental procedure and the analysis of the samples.

3.1 Materials

The sunflower seed shell pellets have an ash content of 4.5 wt% and the ash forming matter composition can be seen in Table 3.2. Sunflower seed shell pellets was chosen since it has been used before in similar experiments in the same reactor, with silica sand as bed material [34].

Element	mg/kg dry fuel
K	8070
Ca	2540
Mg	1900
S	1450
P	522
Cl	390
Si	203
Fe	74.3
Al	56.9
Na	21.3
Sr	18.7
Zn	9.83
Cu	7.71
Mn	6.61
Ti	3.87
Ba	3.43

Table 3.2: Elemental concentrations of the ash forming matter in the sunflower seed shell pellets, including all elements >1 mg/kg dry fuel.

Since the main ash forming element in sunflower seed shell pellets is K, a potassium salt (K_2CO_3) was chosen as a synthetic ash component for the salt experiments. The K_2CO_3 used in the experiments has a purity of 99% and was produced by Fluka.

3.2 Preparation of bed materials

To avoid losing parts of the blast furnace slag bed during the experiments the bed was sifted to remove the smallest fraction. At the same time, the biggest particles were also removed to get a more homogeneous size distribution. A size range of $125 < x < 500$ µm was used as bed material in the reactor.

Oxide scales require pre-treatment before it can be used as bed material since it is contaminated with oil [27]. The oxide scale was therefore heat-treated in an oven at 950°C for 12h to remove the oil. This resulted in sintering of the particles and the material was therefore ground to enable sifting of the material. A size range of $125 < x < 500$ µm was used as bed material, to have the same size range for both materials.

3.3 Fluidized bed reactor

The experiments was performed in a lab scale BFB boiler, which has been used in several previous studies [3, 4, 16, 35]. The reactor is 1.5 m high and consists of three major parts: a pre-heater, a combustion section, and an instrumental and exhaust section, see Figure 3.1. All three parts consist of 4 mm thick AISI 316 steel pipes with an outer diameter of 90 mm and an inner diameter of 82 mm. A tube furnace

is used to heat the pre-heater and the combustion section. The three parts can be dismantled from each other for sampling and cleaning between the experiments [16].

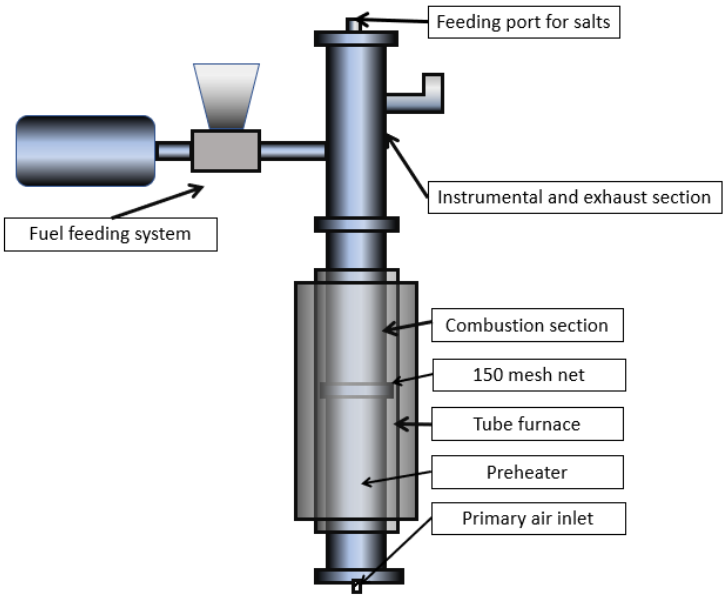

Figure 3.1: Schematics of the reactor used in the experiments.

The air enters the system from the bottom of the pre-heater with a flow rate of about 10 NL/min and is directed towards the walls for more efficient heating. A 150 mesh grid separates the pre-heater from the combustion section and the bed material. When the pre-heated air passes through the mesh grid into the combustion section it fluidizes the bed. The exhaust gases then leave the system through the exhaust channel.

During the experiments, the pressure drop over the bed was monitored. The temperature was measured in the pre-heater, in the bed and in the exhaust gases. Two thermocouples are placed in the bed, at 3.5 cm and 6 cm above the mesh grid. The temperature differences between those two measurements, as well as the pressure drop over the bed, was used to indicate defluidization of the bed. Defluidization causes the pressure drop over the bed to decrease drastically and the difference between the two temperature measurements in the bed to increase. During the experiments, the temperature in the bed was kept at ±10°C from the temperature set for the experiment. The experiments were performed at 850°C and 900°C and 375 g bed material was used in every experiment.

3.3.1 Fuel experiments

For the combustion of solid fuels, a continuous screw feeder was used. When the fuel was added and the combustion started, the furnace temperate needed to be adjusted. When the temperature in the bed occasionally got too high the fuel addition was paused until the temperature was closer to the set temperature. At the same time the furnace heating was decreased to keep the correct temperature in the bed. In case the bed temperature dropped too much the heating was increased.

The experiments were continued until the bed defluidized or until 700 g of fuel had been added.

3.3.2 Salt experiments

The salt was added in batches through a small pipe. The pipe was lowered into the reactor and the salt was injected using three air pulses. The pipe was then removed to avoid eventual blockage of the pipe. Salt was added in 0.5 g batches every 10 minutes and the experiments were continued until defluidization occur or until 10g of salt had been injected.

3.4 Sample preparation

When the reactor had cooled down the remaining bed and potential leftover fuel was collected. Samples from the bed material were cast in epoxy. The epoxy pucks were then polished to reveal smooth surface cross-sections of the samples. A carbon coating was used to avoid surface charges during the SEM-EDX analysis.

3.5 SEM-EDX

Scanning electron microscope (SEM) is an instrument suitable for studying solid sample surfaces. It uses a focused electron beam which scans the sample. By analysis of the backscattering electrons, a very exact image of the topography of the surface can be obtained. To avoid charging of the surface caused by the electron beam, the sample is usually coated with carbon, an alloy, or metal. The coating enables the transport of charges making it possible to get clearer images without disturbance from charges [36, 37].

The SEM does not give information about the chemical content of the sample, but by combining it with an energy-dispersive X-ray (EDX) analyzer chemical information can be obtained. An EDX analyzer analyzes X-rays emitted from the sample when it is hit by the electron beam. The energy of the electron beam is high enough to penetrate the sample and ionize atoms in the sample. When an electron from an inner layer leaves the atom, one from an outer layer will take its place, releasing the specific energy for the transition as an X-ray. Since the energy for the transitions are element-specific, the chemical composition on an elemental basis can be determined from the emitted X-rays. EDX can be used for both qualitative and quantitative analysis [38].

The SEM-EDX analysis together with the pressure and temperature data from the reactor was used to answer the questions presented in section 1.2. Three different kinds of analysis were used: point analysis, line analysis, and map analysis. All map analyses were performed at 250 times magnification and the point analyses at 30 times magnification. Carbon and oxygen will not be presented in the pictures from the map analyses since they are present in the epoxy, but they are accounted for in all calculations.

4

Results

This section will present the results from the eight experiments performed in this project. An overview of the results can be seen in Table 4.1, where the amount fed during the different experiments are listed together with the calculated amount of K it contains, the weight percent of K in the bed, and whether the bed defluidized or not.

Bed	Fuel/salt	Temp (°C)	Defluidized	Amount fed (g)	Amount K fed(g)	K in bed (wt%)
Silica sand	SFSS	900	Yes	91	0.7	0.2
		850	Yes	157	1.2	0.3
	K_2CO_3	900	Yes	3	1.7	0.5
		850	Yes	3.5	2.0	0.5
Blast furnace slag	SFSS	900	No	700	5.2	1.4
		850	No	700	5.2	1.4
	K_2CO_3	900	Yes	7	4.0	1.1
		850	Yes	4.5	2.5	0.7
Oxide Scale	SFSS	900	No	700	5.2	1.4
		850	No	700	5.2	1.4
	K_2CO_3	900	No	10	5.7	1.5
		850	No	10	5.7	1.5

Table 4.1: Results from the eight experiments performed in the project and results from previous studies using silica sand as bed material [16, 34].

4.1 Silica sand

The silica sand used in [16, 34], was not pre-treated before use in the reactor and the bed material can be seen in Figure 4.1.

Figure 4.1: Pictures of silica sand before use in the reactor.

During the combustion of sunflower seed shell pellets the bed defluidized after 157 g and 91 g fuel was fed to the bed at 850°C and 900°C, respectively. This corresponds to 0.3 and 0.2 wt% K in the bed.

The bed also defluidized during the K_2CO_3 addition. K_2CO_3 reacted with the silica sand and formed potassium silicate, causing agglomeration and eventually defluidization. Defluidization occurred after 3.5 g was added at 850°C and after 3 g was added at 900°C. This correlates to a slightly higher K content in the bed (0.5 wt%) compared to the experiments with sunflower seed shell pellets.

4.2 Blast furnace slag

The blast furnace slag used in the experiments was sifted before it was used as bed material. Figure 4.2 shows both the untreated blast furnace slag and the sifted blast furnace slag used in the reactor. The sifted fraction had a particle size of $125 < x < 500$ µm and most of the rejected fraction was particles <125µm.

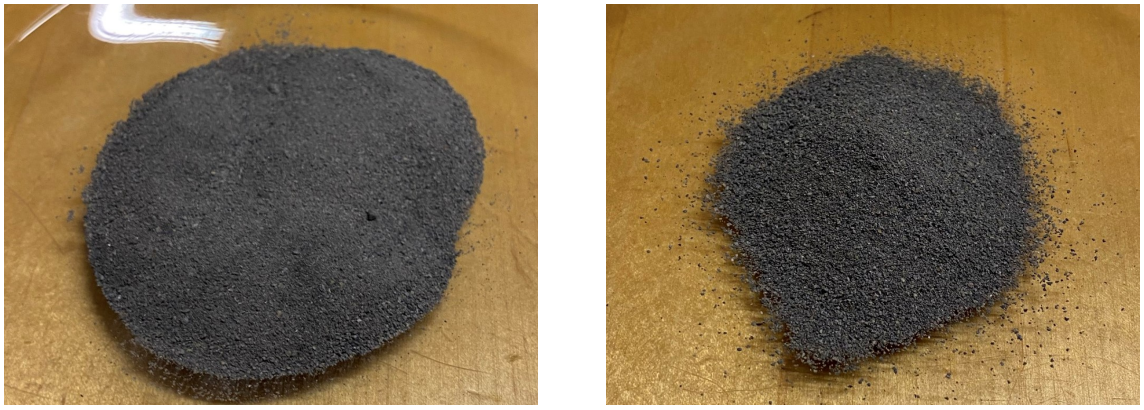

(a) Untreated blast furnace slag **(b)** Sifted blast furnace slag

Figure 4.2: Pictures of blast furnace slag before and after pre-treatment.

The composition of the blast furnace slag was analyzed using SEM-EDX analysis, see Figure 4.3. Figure 4.3 a shows a backscattered SEM image of the sample, where

lighter areas represent heavier elements. Figure 4.3 b-k show representations of the elemental analysis as colored projections onto the back scattered image. The more intense the color, the higher the concentration in the sample. The main components are Al, Ca, Mg, and Si, but it also contains traces of Fe, K, Mn, Na, S, and Ti. The elements are unevenly distributed in the particles and the overall composition can be seen in Appendix B.1.

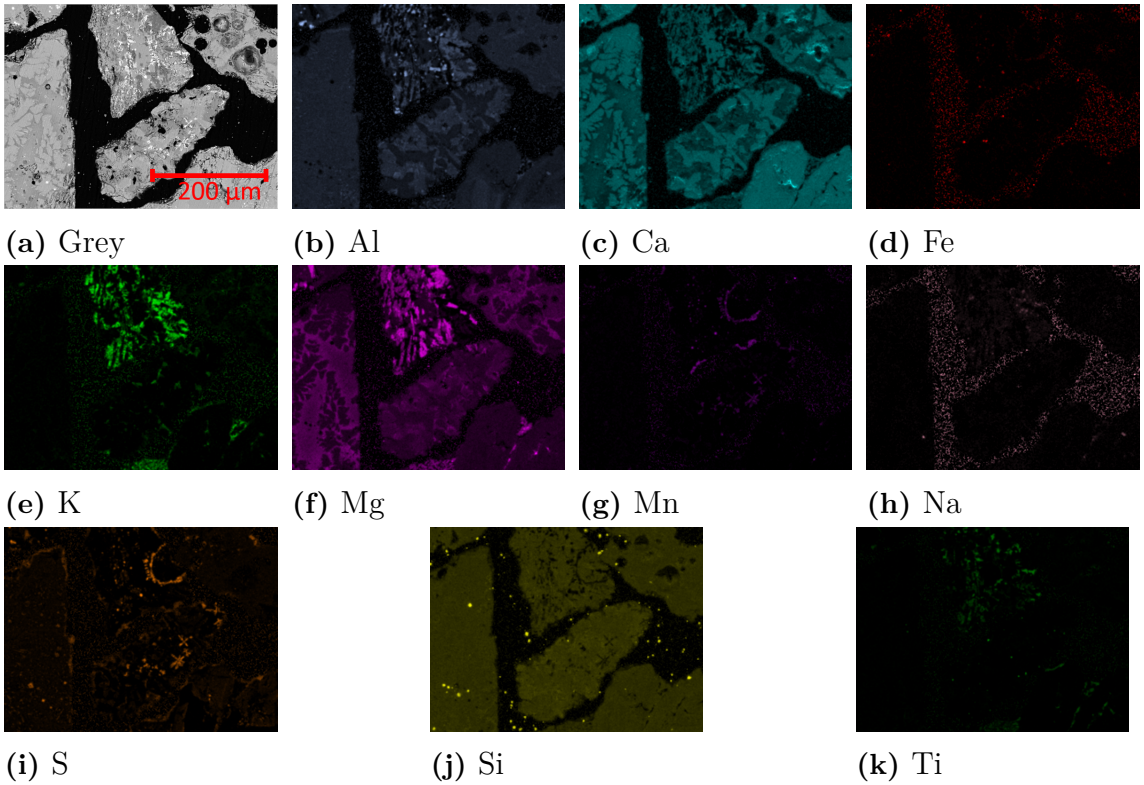

(a) Grey **(b)** Al **(c)** Ca **(d)** Fe

(e) K **(f)** Mg **(g)** Mn **(h)** Na

(i) S **(j)** Si **(k)** Ti

Figure 4.3: a) Backscattered SEM image of blast furnace slag before use in the reactor. b)-k) Representation of the elemental analysis as colored projections.

The analysis of the blast furnace slag also showed that it contains traces of sand particles, see Figure 4.4 and the corresponding Table 4.2.

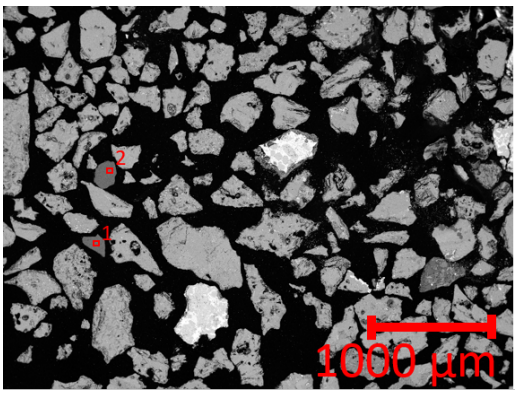

Figure 4.4: Backscattered SEM image of blast furnace slag where number 1 and 2 indicates the sand particles analyzed with point analysis.

Compound	(1) Measured (wt%)	(2) Measured (wt%)
Si	44	42
O	56	58

Table 4.2: Composition of the sand particles marked as 1 and 2 in Figure 4.4.

4.3 Blast furnace slag after sunflower seed shell pellets combustion

When blast furnace slag was used as bed material during the combustion of sunflower seed shell pellets, round agglomerates formed in the bed. The bed also went from the grey color of the raw material (Figure 4.2) to brown, see Figure 4.5. There were more and larger agglomerates in the bed after combustion at 900°C.

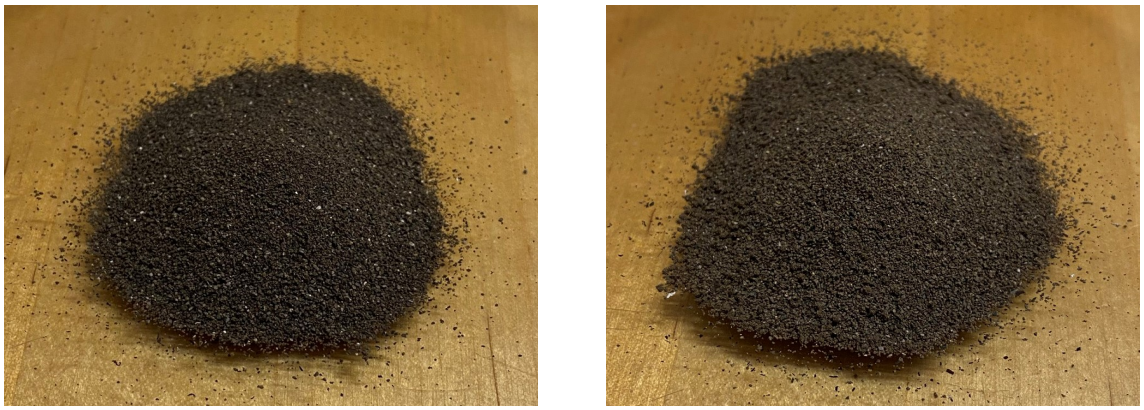

(a) 850°C **(b)** 900°C

Figure 4.5: Pictures of blast furnace slag after combustion of sunflower seed shell pellets at 850°C and 900°C.

During the experiments, 700 g sunflower seed shell pellets were added to the reactor before the experiment was ended. The pressure over the bed as well as the difference between t1 and t2 (the temperatures measured 3.5 cm respective 6 cm above the mesh grid in the reactor) were quite stable during the entire experiment, which indicates that the bed did not defluidize, see Figure 4.6. The temperature of the exhaust gas (t3) decreases when the combustion begins.

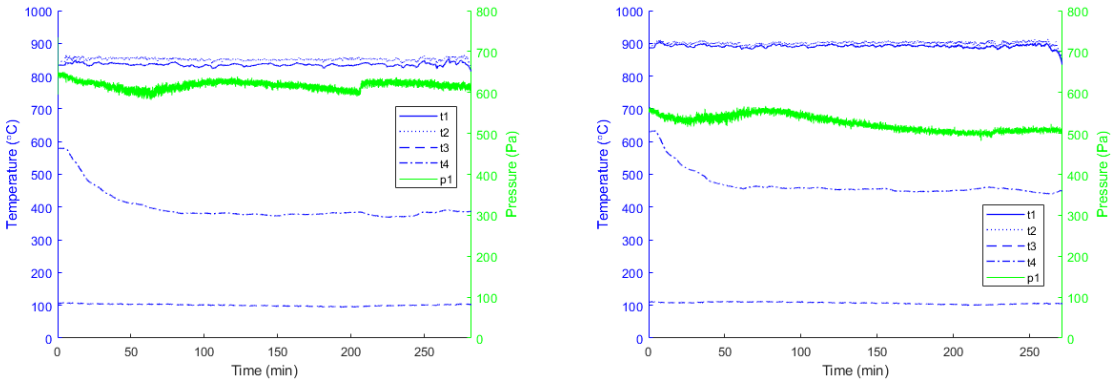

(a) 850°C **(b)** 900°C

Figure 4.6: Temperature and pressure measurements for combustion of sunflower seed shell pellets in a blast furnace slag bed at 850°C and 900°C. t1 and t2 are the temperatures 3.5 cm respective 6 cm above the mesh grid in the reactor. t3 is the temperature of the exhaust gas, t4 the temperature of the air entering the reactor, and p1 the pressure drop over the bed.

SEM-EDX analysis of the agglomerates showed that they were built up around a sand particle core surrounded by the typical blast furnace slag particles. The particles are glued together by potassium silicate, see Figure 4.7. All images from the analysis of both temperatures can be seen in Appendix A.1.1.

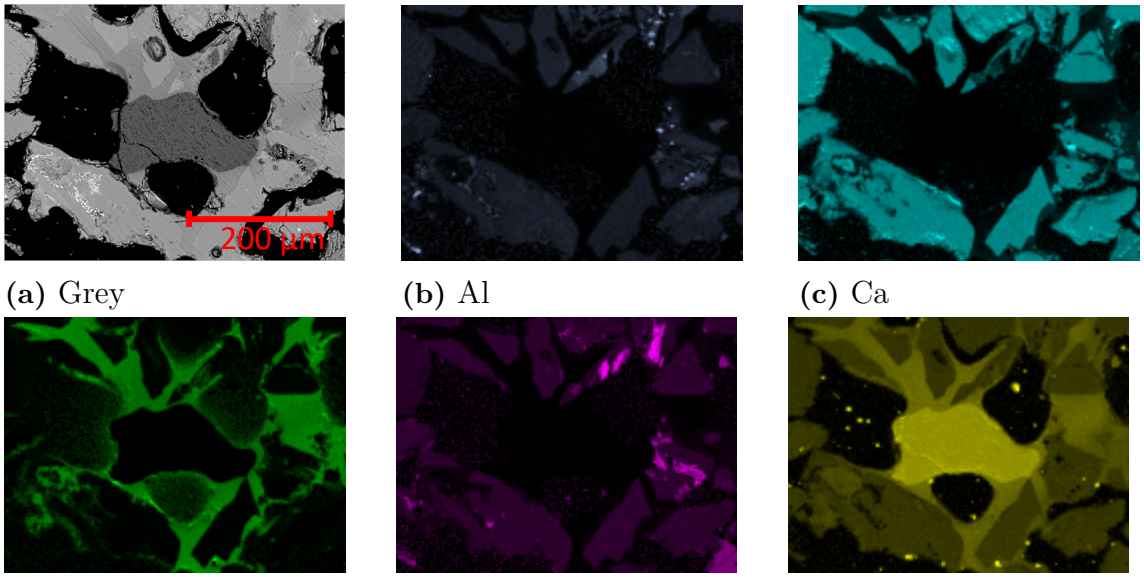

(a) Grey **(b)** Al **(c)** Ca

(d) K **(e)** Mg **(f)** Si

Figure 4.7: Major elements of a agglomerate from the blast furnace slag bed after sunflower seed shell pellets combustion at 900°C.

The elemental analysis along the arrow of the agglomerate in Figure 4.8 shows five different regions. First the epoxy, only containing carbon and oxygen (the black parts in the image). Then a thin layer around 20 µm with a high K content at the

surface of the particle (25-70 µm), which contains Al, Ca, Mg, and Si. There is a clear decrease of most of the components from the particle where the "glue" (70-90 µm), consisting of potassium silicate begins and the arrow ends in the silica oxide (sand particle) in the middle of the agglomerate.

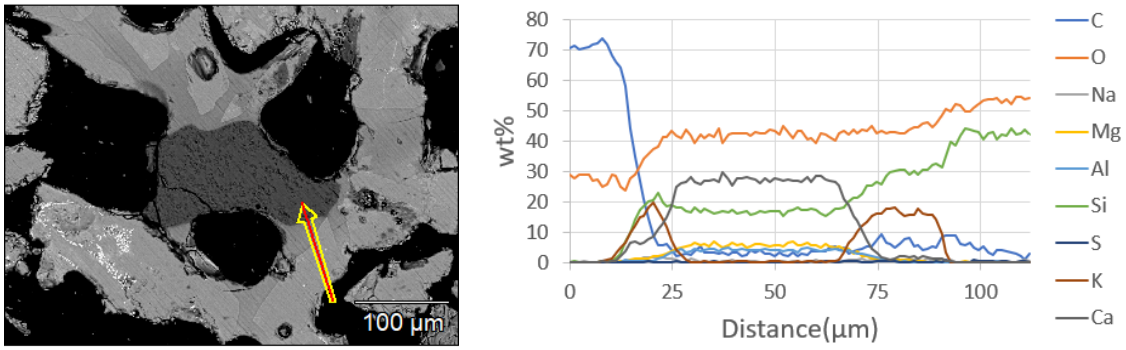

Figure 4.8: Elemental analysis along the arrow of the agglomerate from Figure 4.7.

4.4 Blast furnace slag after K_2CO_3 addition

When K_2CO_3 was added to the bed, agglomerates were formed, see Figure 4.9. The bed had a similar color as after the combustion of sunflower seed shell pellets, but when K_2CO_3 was added, the bed also contained white particles, see Section 4.8.

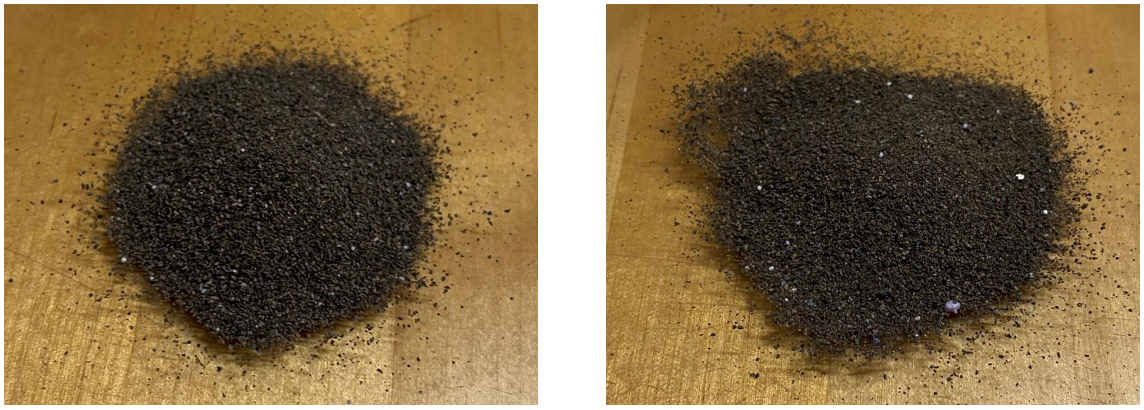

(a) 850°C **(b)** 900°C

Figure 4.9: Pictures of blast furnace slag after addition of K_2CO_3 at 850°C and 900°C.

The K_2CO_3 was added using air pulses every 10 minutes, which can be seen as fluctuations in both the temperature and pressure measurements in Figure 4.10. At both temperatures, a major change in the pressure difference over the bed was observed before the experiments were ended. The sudden decrease was caused by the defluidization of the bed, which occurred after 4.5 g K_2CO_3 was added at 850°C and 7.5 g K_2CO_3 at 900°C.

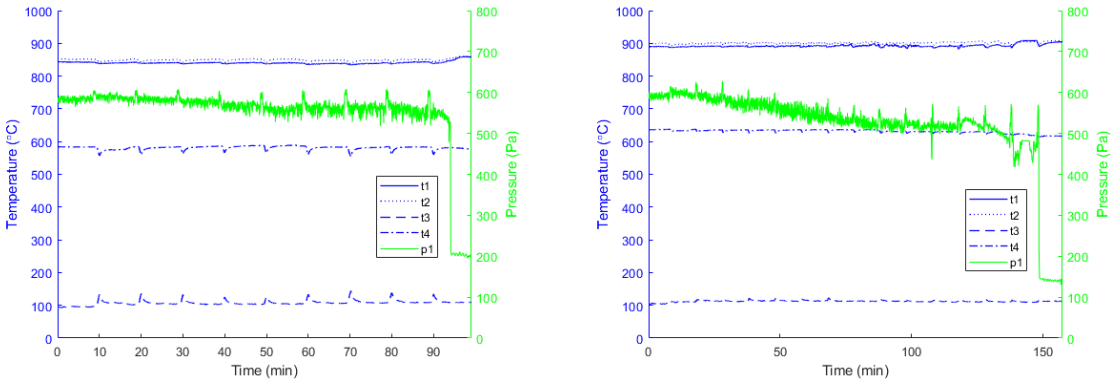

(a) 850°C **(b)** 900°C

Figure 4.10: Temperature and pressure measurements during addition of K_2CO_3 to a blast furnace slag bed at 850°C and 900°C. t1 and t2 are the temperatures 3.5 cm respective 6 cm above the mesh grid in the reactor. t3 is the temperature of the exhaust gas, t4 the temperature of the air entering the reactor, and p1 the pressure drop over the bed.

The backscattered SEM images did not show any agglomerates in the bed from 850°C and therefore only a map of normal particles are presented for this temperature in Appendix A.1.2. The agglomerates from the 900°C bed were built up around sand particles and the surrounding particles mainly contained Al, Ca, Mg, and Si, see Figure 4.11. Some particles have a K and S layer, but there is nearly no S around the sand particle. There is also some Si between the particles. All images from the analysis of both temperatures can be seen in Appendix A.1.2.

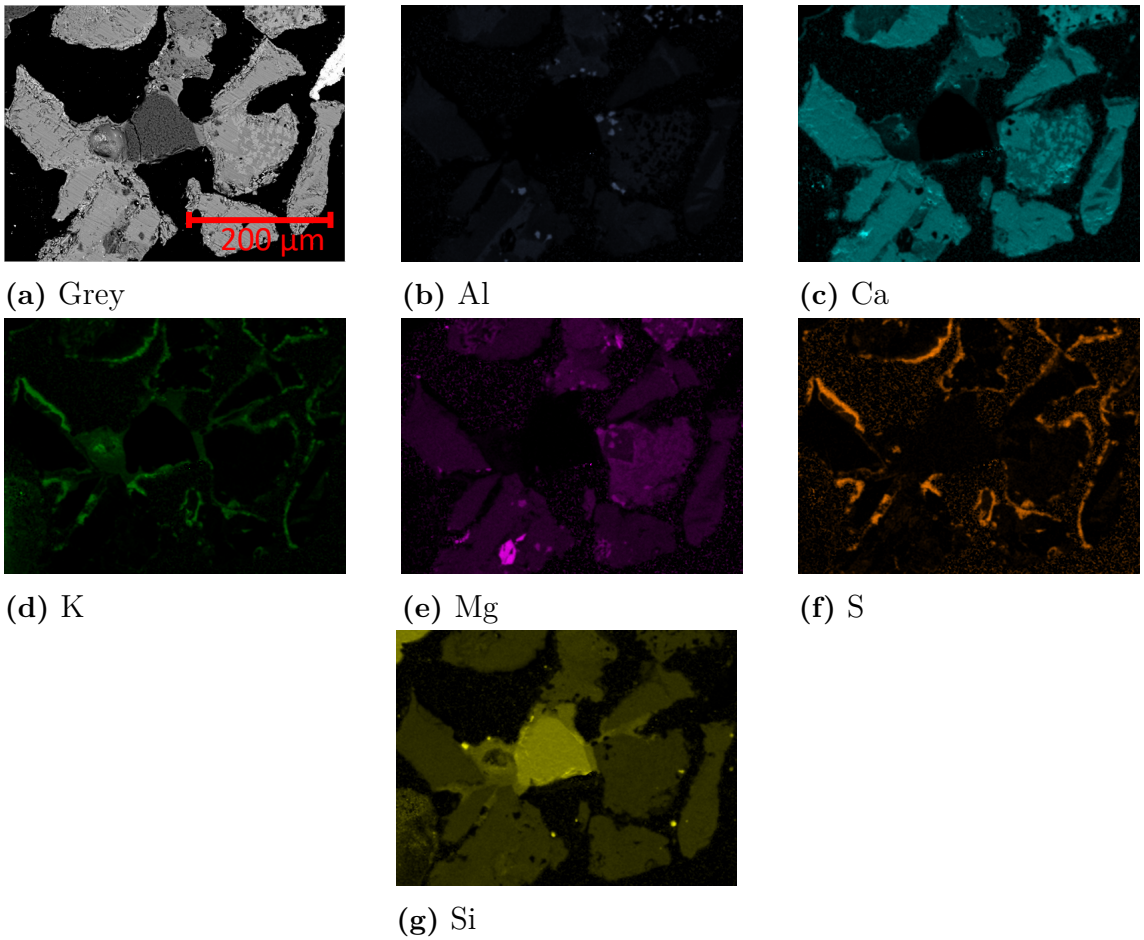

(a) Grey **(b)** Al **(c)** Ca

(d) K **(e)** Mg **(f)** S

(g) Si

Figure 4.11: Major elements of a agglomerate from the blast furnace slag bed after K_2CO_3 addition at 900°C.

The elemental analysis along the arrow of the agglomerate in Figure 4.12, shows that the "glue" between the sand particle in the middle and one of the other particles consists of potassium silicate. There is a clear peak in the K content around 15-25 µm where the Si content starts to drop indicating the edge between the sand particle and the other particle. The other particles have a composition typical for the blast furnace slag.

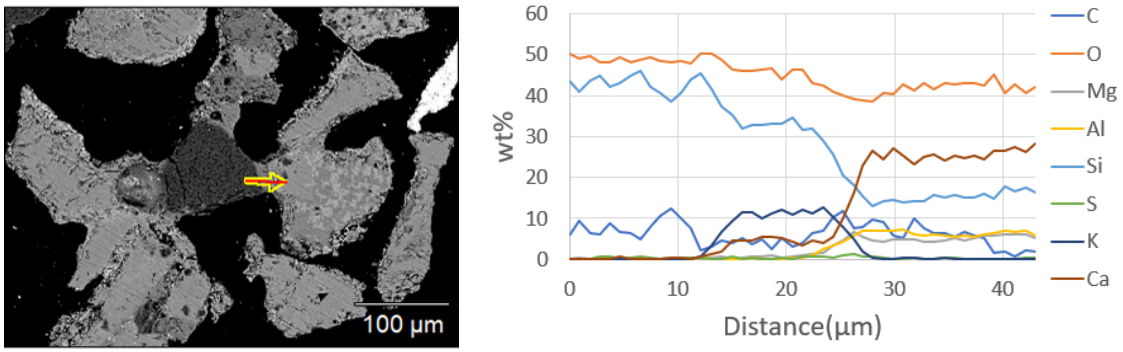

Figure 4.12: Elemental analysis along the arrow of the agglomerate from Figure 4.11.

Further out in the agglomerate, where the S and K layers can be seen in Figure 4.11 another elemental analysis was performed along the arrow in Figure 4.13. The arrow goes through three different particles and two segments of "glue", see Figure. The "glue" is characterized by the increase of K and S around 35 and 75 µm.

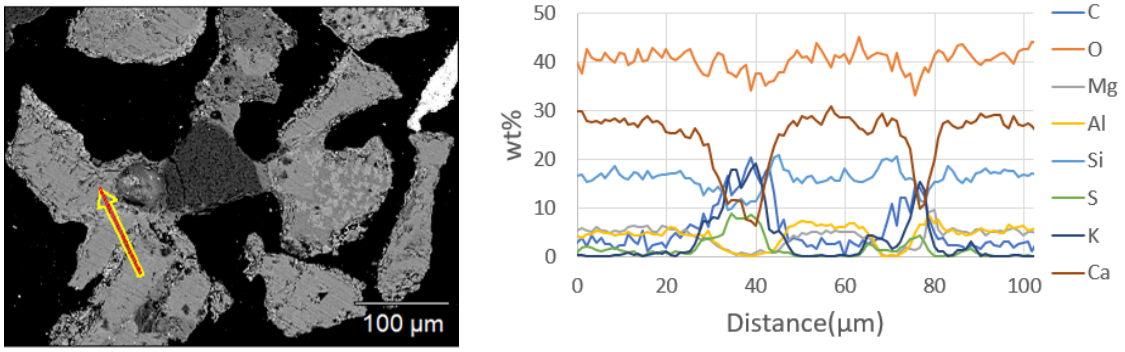

Figure 4.13: Elemental analysis along the arrow of the agglomerate from Figure 4.11.

4.5 Oxide scale

Oxide scales were heat-treated in an oven, grinded, and sifted before use in the reactor. Figure 4.14 show the oxide scales before and after pre-treatment.

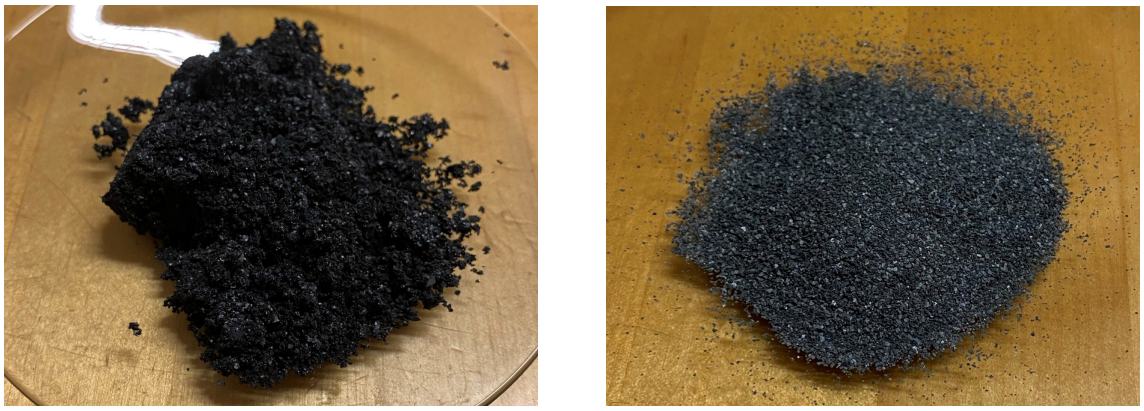

(a) Untreated oxide scales **(b)** Pre-treated oxide scales

Figure 4.14: Pictures of oxide scales before and after pre-treatment.

The elemental analysis show that the oxide scales consists of almost only iron oxide, but it also contains small traces of Al, Ca, Cr, Mn, and Si, see Figure 4.15. The composition of the oxide scale can be seen in Appendix B.2.

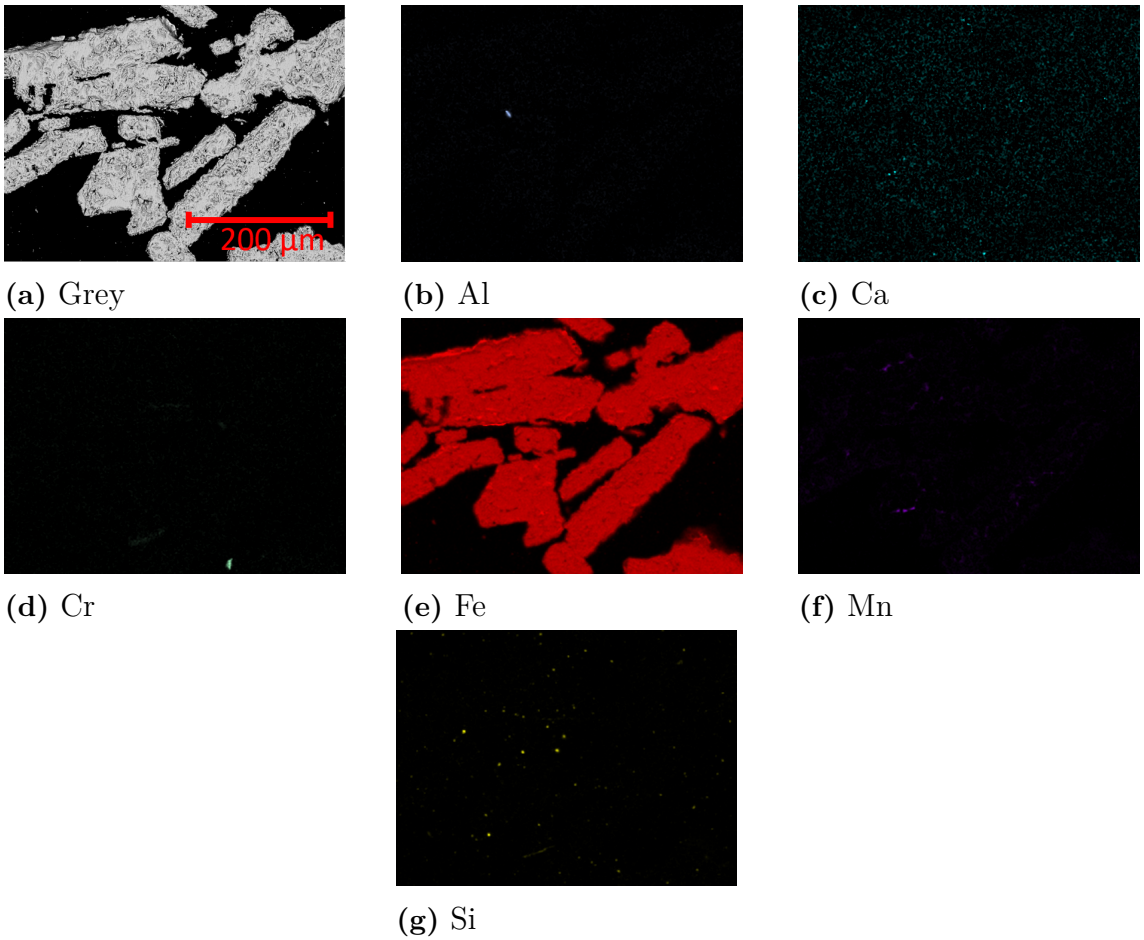

(a) Grey **(b)** Al **(c)** Ca

(d) Cr **(e)** Fe **(f)** Mn

(g) Si

Figure 4.15: a) Backscattered SEM image of oxide scale before use in the reactor. b)-g) Representation of the elemental analysis as colored projections.

4.6 Oxide scale after sunflower seed shell combustion

During the combustion of sunflower seed shell pellets, the bed material changed from the grey color of the pre-treated material to a red powder containing some grey particles, see Figure 4.16.

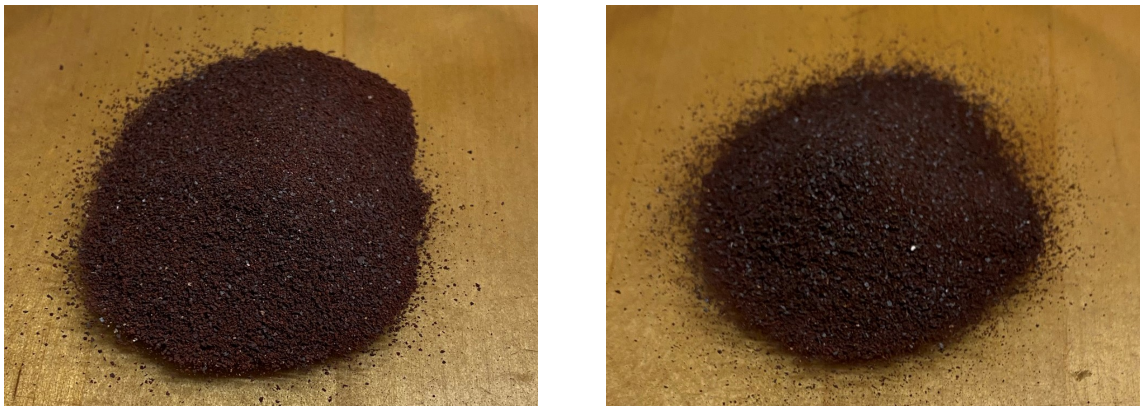

(a) 850°C **(b)** 900°C

Figure 4.16: Bed material after use in the reactor.

700 g of sunflower seed shell pellets was added to the reactor. The pressure over the bed and the difference between t1 and t2 stayed quite stable during the experiment, indicating that no defluidization occurred, see Figure 4.17. Similar to the experiments where sun flower peel pellets were combusted in the blast furnace slag bed, t3 decreases when the combustion starts. During the combustion using the oxide scale bed, the temperature was less stable than for the other experiments performed. Small changes in the oven temperature could cause much larger changes in the bed temperature, resulting in a less stable temperature throughout the experiment. This is visible in the much larger variations of t1 and t2 in Figure 4.17 compared to the other experiments performed.

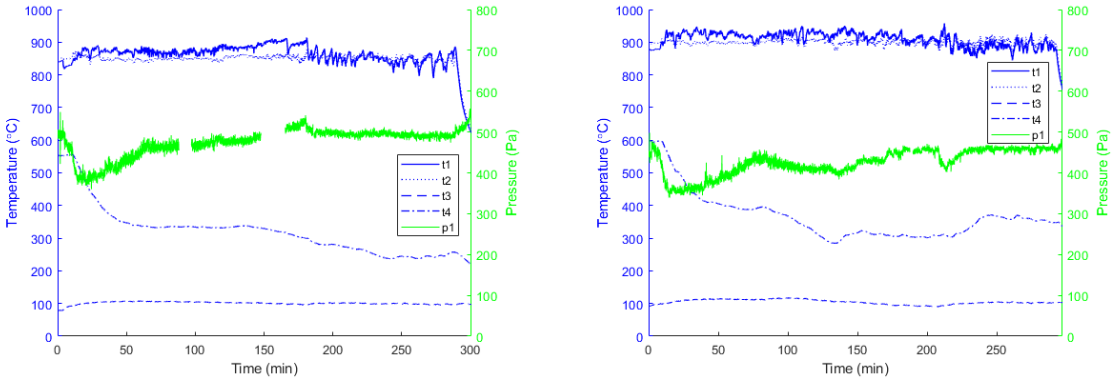

(a) 850°C **(b)** 900°C

Figure 4.17: Temperature and pressure measurements for combustion of sunflower seed shell pellets in an oxide scale bed at 850°C and 900°C. t1 and t2 are the temperatures 3.5 cm respective 6 cm above the mesh grid in the reactor. t3 is the temperature of the exhaust gas, t4 the temperature of the air entering the reactor and p1 the pressure drop over the bed. The gaps in the pressure curve of a) are due to periods of connection problems with the instrument measuring the pressure.

The elemental analysis of the agglomerates showed that the main element in the particles is Fe, see Figure 4.18. K is gathered around the agglomerates and only

small amounts of potassium silicate were found. The particles seem to have a more porous structure after the combustion of sunflower seed shell pellets compared to the other experiments. All images from the analysis of both temperatures can be seen in Appendix A.2.1.

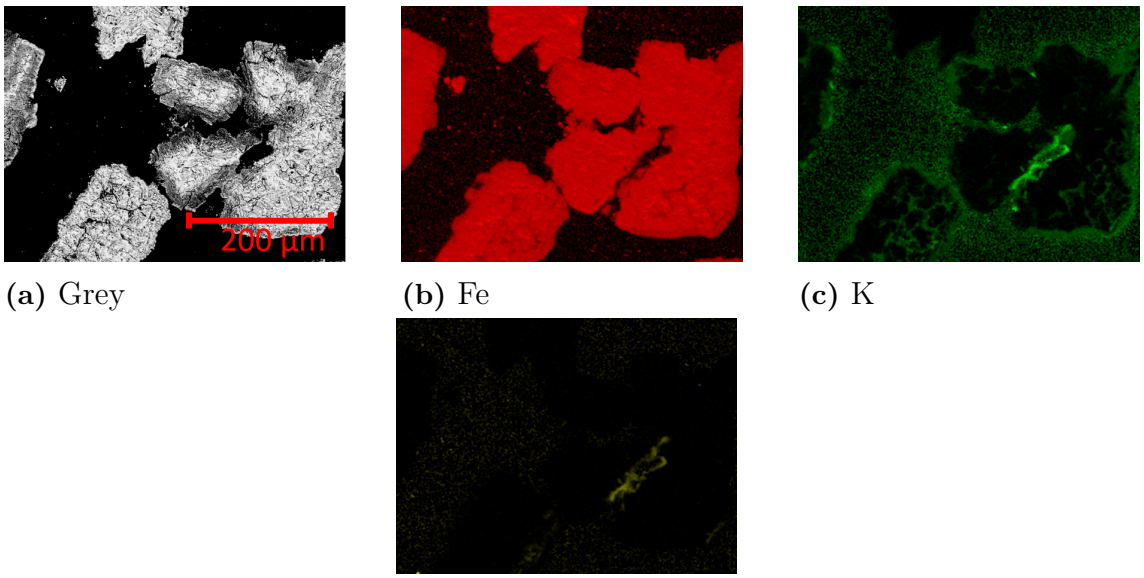

(a) Grey **(b)** Fe **(c)** K

(d) Si

Figure 4.18: Major elements of an agglomerate from the oxide scale bed after K_2CO_3 addition at 900°C.

Most of the boundaries between the different particles in the agglomerate showed no traces of other elements than Fe, see Figure 4.19. The Fe and O content are nearly stable at the boundary between the two particles and the C present in the analysis is from the carbon coating added before the SEM-EDX analysis.

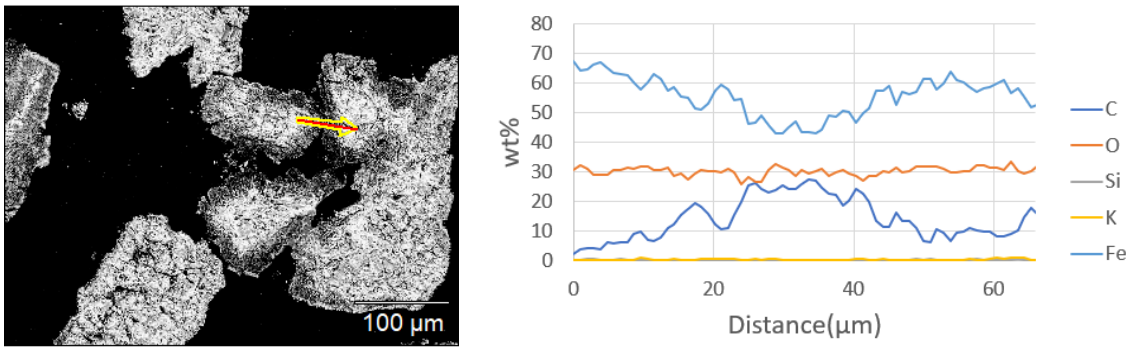

Figure 4.19: Elemental analysis along the arrow of the agglomerate from Figure 4.18.

There are also a few examples found where some potassium silicate can be found at the boundary between the particles, see Figure 4.20.

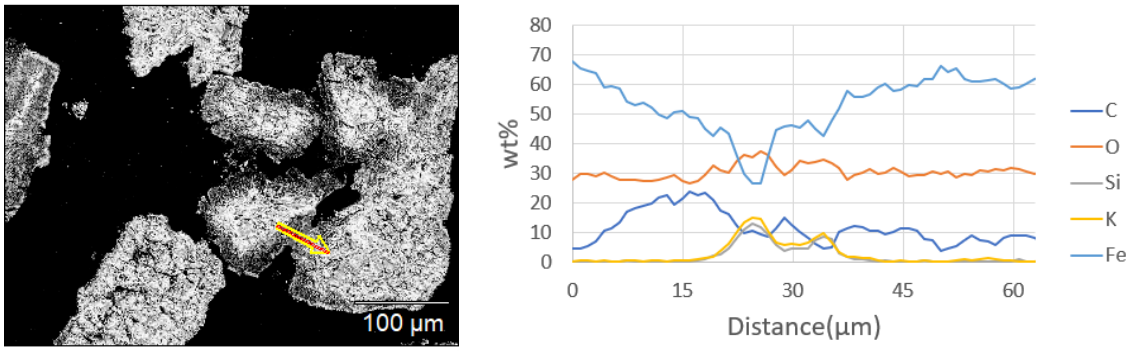

Figure 4.20: Elemental analysis along the arrow of the agglomerate from Figure 4.18.

4.7 Oxide scale after K_2CO_3 addition

After adding K_2CO_3 to the oxide scale bed the resulting bed particles were darker than before the experiment, see Figure 4.21. White particles were also found in the bed, see Section 4.8.

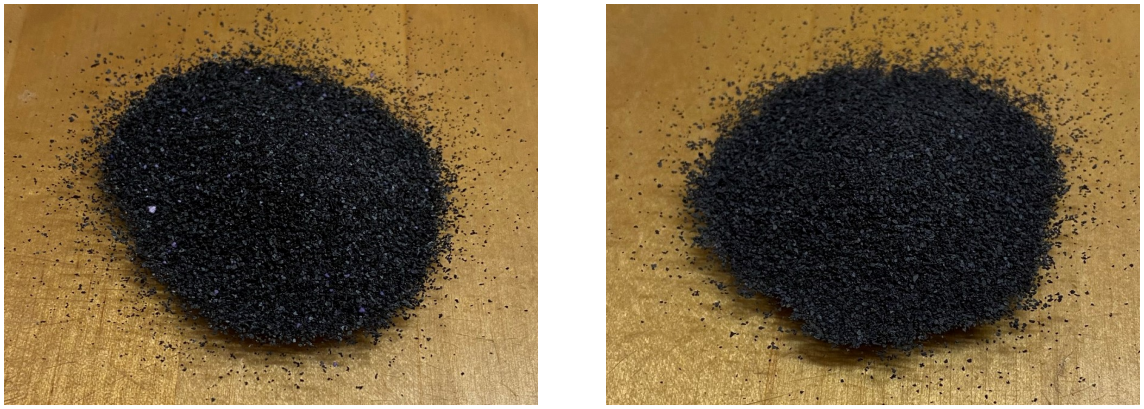

(a) 850°C **(b)** 900°C

Figure 4.21: Oxide scales after addition of K_2CO_3 at 850°C and 900°C.

When K_2CO_3 was added to an oxide scale bed the pressure difference and the difference between t1 and t2 was quite constant during the entire experiments, indicating that no defluidization occurred, see Figure 4.22. A total amount of 10 g K_2CO_3 was added during the experiments at both temperatures.

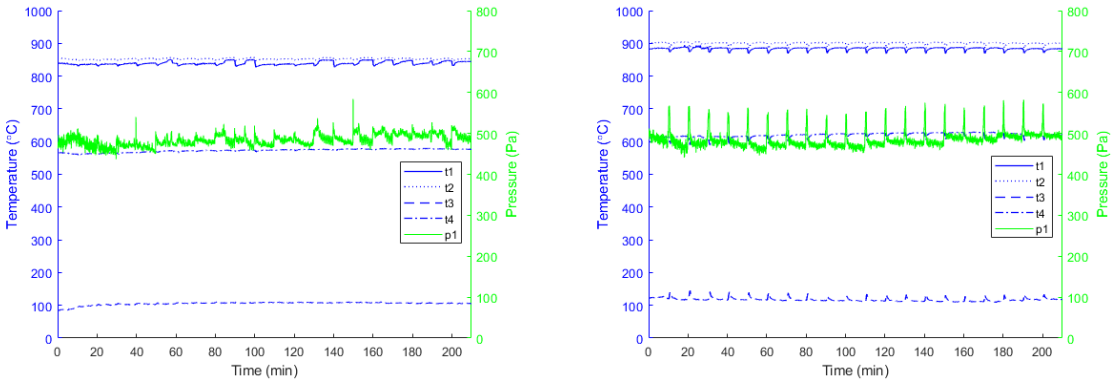

(a) 850°C **(b)** 900°C

Figure 4.22: Temperature and pressure measurements during addition of K_2CO_3 to an oxide scale bed at 850°C and 900°C. t1 and t2 are the temperatures 3.5 cm respective 6 cm above the mesh grid in the reactor. t3 is the temperature of the exhaust gas, t4 the temperature of the air entering the reactor, and p1 the pressure drop over the bed.

When the elemental compositions of the agglomerates were analyzed, the particles mainly contained Fe and some K had gathered around the agglomerates, see Figure 4.23. All images from the analysis of both temperatures can be seen in Appendix A.2.2.

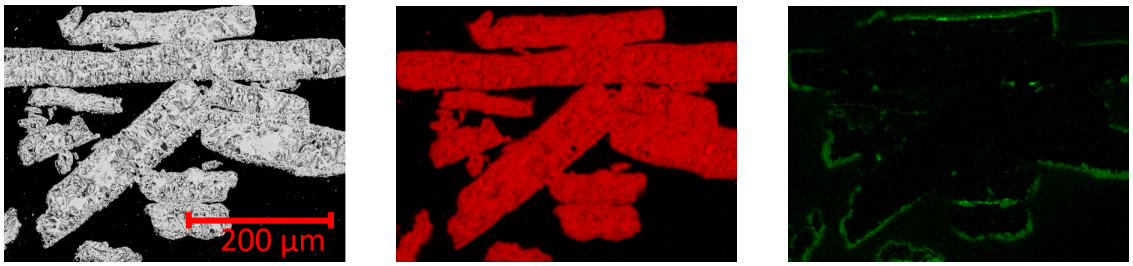

(a) Grey **(b)** Fe **(c)** K

Figure 4.23: Major elements of a agglomerate from the oxide scale bed after K_2CO_3 addition at 900°C.

The elemental analysis along the arrow of the agglomerate shows a constant concentration of Fe and O throughout the entire agglomerate, see Figure 4.24.

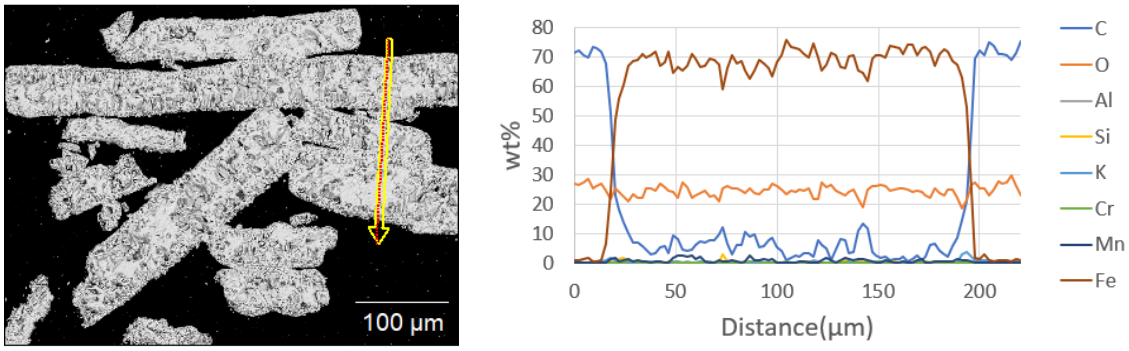

Figure 4.24: Elemental analysis along the arrow of the agglomerate from Figure 4.23.

4.8 White particles

The white particles found in the bed after K_2CO_3 addition to both bed materials were also analyzed using point analysis. The particles were found to be round shapes like the particles marked in Figure 4.25. The analysis of the points in Figure 4.25 (a) and (b) are presented as the measured values in Table 4.3 together with the theoretical values for K_2CO_3.

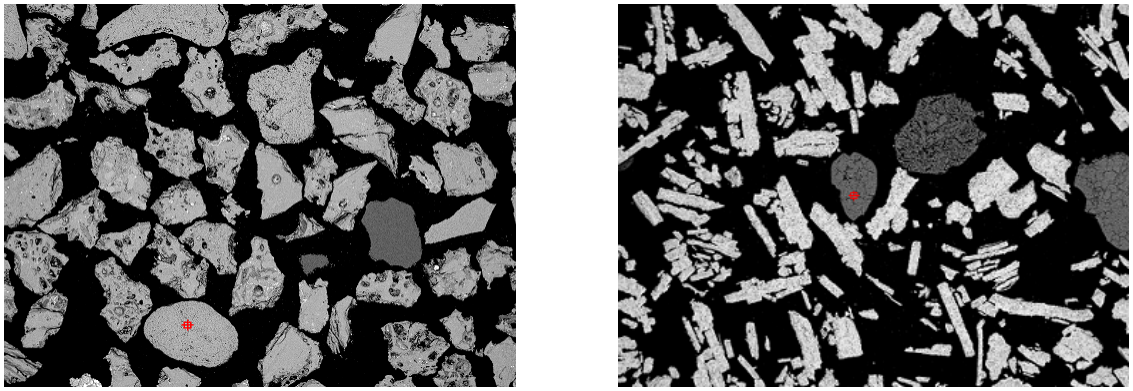

(a) Blast furnace slag **(b)** Oxide scales

Figure 4.25: Backscattered SEM images of the white particles found after K_2CO_3 addition to both bed materials.

Compound	(a) Measured (at%)	(b) Measured (at%)	K_2CO_3 (at%)
K	27	24	33
C	23	23	16
O	49	53	50
Na	0.6	-	-
Si	-	0.2	-

Table 4.3: Composition of the particles marked in Figure 4.25 (a) and (b) compared to theoretical values for K_2CO_3.

5
Discussion

The two materials tested in this study were also compared to previous studies performed with silica sand. In this study, both bed materials were pre-treated before use in the reactor, while the silica sand from previous studies was not. The blast furnace slag was only pre-treated to avoid an excessive loss of smaller bed particles but could be used without pre-treatment. Oxide scales required pre-treatment to remove the oil residue from the material. The heat-treatment and the grinding needed would complicate the use in an industrial-scale reactor, making the material more expensive to use. Therefore it would be interesting to investigate whether it would be possible to remove the oil by adding the raw material to the bed during the combustion. This way only the material used for starting the process would need pre-treatment, but this would require further investigation.

During the experiments with the blast furnace slag bed, the bed particles form visible agglomerates. The SEM-EDX analysis of the agglomerates shows that they form around sand particles. Since there are sand particles present in the blast furnace slag it is most likely those particles that can be seen in the agglomerates. During the combustion of sunflower seed shell pellets, the agglomerates are held together by potassium silicate, which is known to act as a glue and therefore causes agglomeration. That the agglomerates form around the sand particles could indicate that the potassium silicate layer gets thicker around the sand particles and that other particles get stuck in the glue when they collide with the sand particles in the bed. This would explain the form of the particles but would need to be examined further to prove accurate.

The agglomeration seems to be layer-induced, meaning that the K from the fuel reacts with the Si in the bed material forming sticky potassium silicate layers on the particles. The fact that nearly no potassium silicate was found in the oxide scale bed after the combustion of the same amount of fuel, also strengthens the theory that it was not melt-induced. If it was melt-induced and both the K and the Si causing the agglomeration originated from the fuel a similar amount of potassium silicate should have been found in the oxide scale bed. This indicates that the amount of Si added to the bed by the fuel combustion would not be enough to cause as much agglomeration as was observed in the blast furnace slag bed. Therefore it is reasonable to conclude that the K reacted with the Si in the bed particles, causing layer-induced agglomeration.

During the experiments with K_2CO_3 addition to the blast furnace slag bed, the agglomerates are similar to the ones received during sunflower seed shell pellets combustion. Similar potassium silicate layers are formed around the sand particles in the middle of the agglomerates. The difference is that the other particles have

layers consisting of K and S instead of K and Si as in the sunflower seed shell pellets experiments. Since the only thing added to the bed is K_2CO_3 the S must originate from the blast furnace slag. Before the use in the reactor, some S was found unevenly distributed in the blast furnace slag particles, see Figure A.1. Then after the K_2CO_3 addition experiments, the S is instead found in the layers around the particles indicating that the S migrates to the surface of the particle during the time in the reactor. It then forms a layer together with the K from the added salt, see Figure A.5. If the S migrates to the surface and how it interacts with K would need to be further investigated.

During the study, the addition of K_2CO_3 to the blast furnace slag bed generated the only defluidization within the set limits for addition, indicating that the oxide scales can withstand a higher K content before defluidization. Still, the salt experiments are only a simplified version of biomass combustion and to know more about how the bed materials could handle an actual fuel like the sunflower seed shell pellets the experiments with the fuel would have had to continue until defluidization. This was unfortunately not possible in this project since the length of every experiment was limited to what could be performed in one workday. The experiments also indicated that more K was needed to defluidize the bed at 900°C than at 850°C. This is the opposite from the results from previous studies with silica sand. This could possibly be caused by some error during the experiment and the experiments should therefore be repeated before any conclusions are drawn from this.

The oxide scale bed is very different from the other bed materials since it can act as an oxygen carrier in the bed and thereby aid the combustion more. SEM-EDX analysis of the sample before use in the reactor showed that it consists of iron oxide with only small traces of other compounds, see Figure A.6. It also showed that some of the particles are still attached to each other indicating that there are still some agglomerates caused by the heat-treatment left after the grinding of the material. This is the same kind of agglomerates that can be seen in the bed after both sunflower seed shell pellets combustion and K_2CO_3 addition.

The line scans of the agglomerates indicate that the composition of the particles in the agglomerates is the same even at the boundary between the particles in the oxide scale beds. K added during the experiments only gather at the surface of those agglomerates. Only one exception was found during the analysis of the oxide scale samples when some potassium silicate was found in the sample after sunflower seed shell pellets combustion at 900°C. The small amount of Si found most likely originates from the sunflower seed shell pellets which contain 203 mg Si/kg dry fuel. This indicates that the Si from the sunflower seed shell pellets potentially could cause agglomeration, but that the effect of it was barely noticeable in the sample after the addition of 700 g, indicating that much larger amounts would be needed to get a significant effect of the formed potassium silicate.

During the combustion experiments with sunflower seed shell pellets in the oxide scales bed, the temperature was fluctuating more than for the other samples. When the temperature was adjusted a few degrees the actual temperature inside the reactor could change a lot more. This unstable system could be the result of oxidation and reduction processes in the bed, which could occur if the combustion were close to the stoichiometric conditions. The C, H, and O content of the sunflower seed shell

pellets would have been needed to calculate whether the combustion was close to the stoichiometric point. That would enable a change between oxidizing and reductive atmosphere in the reactor caused by small changes in the temperature.

During the project the oxide scale bed displayed a variety of colors, starting with the dark oily mass with grey metal glance particles of the raw material that turned a lighter gray after the pre-treatment. Then during the time in the reactor, the color changed again to a red powder with some grey particles after sunflower seed shell pellets combustion and darker gray particles after the K_2CO_3 addition. It would have been interesting to further examine what caused the color changes.

During this study, the behavior of exhaust gas temperature was the same for both bed materials but showed a clear difference between the experiments with sunflower seed shell pellets combustion and the experiments with K_2CO_3 addition. During the K_2CO_3 addition the exhaust gas temperature was stable for both bed materials, but during the sunflower seed shell pellets combustion, the temperature declined significantly before stabilizing at a much lower temperature than for the salt experiments. This is most likely caused by the additional heat originating from the combustion, which required a lower oven temperature to maintain the set temperature inside the reactor. The lower oven temperature will result in a lower temperature of the steel pipe of the exhaust section since less heat will be transported there, resulting in a cooling effect on the exhaust gas.

Another thing that both bed materials had in common is that white particles could be found in both bed materials after the K_2CO_3 addition. The SEM-EDX analysis of those particles indicates a composition very close to the composition of K_2CO_3 with only very small traces of other compounds, making it a reasonable assumption that the particles are made up by K_2CO_3. How and why those particles were formed has not been examined in this project, but could potentially be the result of partial or entire melting of the salt particles upon entering the reactor and then sticking together forming those bigger particles.

When the three materials are compared it is clear that silica sand defluidized at a lower K content in the bed than both blast furnace slag and oxide scale. That the blast furnace slag bed defluidized during the salt experiments while the oxide scale bed did not indicates that the oxide scale bed can handle higher K content in the bed without defluidization. This indicates that oxide scale is the best bed material in this study to counteract defluidization for fuels with a high K content. Still, the fact that oxide scale would require pre-treatment is something that needs to be considered, since it would increase the cost. The benefits of the material would therefore need to be compared to the cost.

One potential source of error in the experiments is the cooling of the pipe used for the salt addition to the bed. After the pipe is removed from the reactor, the air flow is opened slightly to let the airflow cool down the pipe. This is done to prevent clogging of the pipe. When the airflow is opened it also increases the flow through the reactor which is linked to the same pressure air system. The increased airflow through the reactor could potentially have some effect on the results of the salt experiments, but further examination would be needed to examine the potential effects on the results. Because of the time limitation for the project most of the experiments were only conducted once, which makes it possible that human error

could affect the results.

6
Conclusion

Blast furnace slag forms agglomerates caused by the potassium silicate layer built up on the particles during both sunflower seed shell pellets combustion and K_2CO_3 addition. The agglomerates form around sand particles in the bed indicating that the sand particles play an important role in the agglomeration. During the experiments with K_2CO_3 addition to the blast furnace slag bed, S and K layers formed around the non-sand particles in the agglomerates. The S also seemed to migrate to the surface during the time in the reactor.

Oxide scales barely form any new agglomerates during the time in the reactor. Instead, K gathers around the particles and agglomerates from the pre-treatment. Some traces of potassium silicate was found in the bed after sunflower seed shell pellets combustion. This indicates that the Si from the sunflower seed shell pellets could potentially cause more agglomeration at higher concentrations.

The temperature in the bed was less stable during the sunflower seed shell pellets combustion in the oxide scale bed compared to the other experiments. This could potentially be caused by the combustion taking place close to stoichiometric conditions.

When comparing the two bed materials used in this project with the results from previous studies using silica sand, the silica sand agglomerates at the lowest K concentration, followed by blast furnace slag. Oxide scales seem to be the most resistant towards agglomeration in this comparison. This could potentially be related to the silica content of the bed material.

Before using blast furnace slag or oxide scales in an industrial-scale fluidized bed, there are of course many more things to consider. But the results from this study indicate that oxide scale is the most K-resistant when it comes to agglomeration. Still, the fact that it requires pre-treatment could be a problem in industrial-scale use, especially since it would increase the cost of the material. The advantages of the material would therefore need to be compared to the cost.

Bibliography

[1] M. Rydén, M. Hanning, and F. Lind, "Oxygen Carrier Aided Combustion (OCAC) of wood chips in a 12 MWth circulating fluidized bed boiler using steel converter slag as bed material", *Applied Sciences (Switzerland)*, vol. 8, no. 12, 2018, ISSN: 20763417. DOI: 10.3390/app8122657.

[2] J. Koornneef, M. Junginger, and A. Faaij, "Development of fluidized bed combustion—an overview of trends, performance and cost", *Progress in Energy and Combustion Science*, vol. 33, no. 1, pp. 19–55, 2007, ISSN: 0360-1285. DOI: https://doi.org/10.1016/j.pecs.2006.07.001. [Online]. Available: https://www.sciencedirect.com/science/article/pii/S0360128506000335.

[3] C. Sevonius, P. Yrjas, D. Lindberg, and L. Hupa, "Agglomeration tendency of a fluidized bed during addition of different phosphate compounds", *Fuel*, vol. 268, no. January, 2020, ISSN: 00162361. DOI: 10.1016/j.fuel.2020.117300.

[4] M. Zevenhoven, C. Sevonius, P. Salminen, D. Lindberg, A. Brink, P. Yrjas, and L. Hupa, "Defluidization of the oxygen carrier ilmenite – Laboratory experiments with potassium salts", *Energy*, vol. 148, pp. 930–940, 2018, ISSN: 03605442. DOI: 10.1016/j.energy.2018.01.184. [Online]. Available: https://doi.org/10.1016/j.energy.2018.01.184.

[5] A. A. Khan, W. de Jong, P. J. Jansens, and H. Spliethoff, "Biomass combustion in fluidized bed boilers: Potential problems and remedies", *Fuel Processing Technology*, vol. 90, no. 1, pp. 21–50, 2009, ISSN: 03783820. DOI: 10.1016/j.fuproc.2008.07.012.

[6] A. Gyllén, *THESIS FOR THE DEGREE OF DOCTOR OF PHILOSOPHY Oxygen carrier aided combustion: Implementation of oxygen carriers to existing industrial settings*. 2019, ISBN: 9789179051242. [Online]. Available: https://research.chalmers.se/publication/510067/file/510067%7B%5C_%7DFulltext.pdf.

[7] T. Pröll, "Fundamentals of chemical looping combustion and introduction to CLC reactordesign", in *Calcium and Chemical Looping Technology for Power Generation and Carbon Dioxide (CO*, Elsevier Inc., 2015, pp. 197–219, ISBN: 9780857097606. DOI: 10.1016/B978-0-85709-243-4.00010-0.

[8] H. Thunman, F. Lind, C. Breitholtz, N. Berguerand, and M. Seemann, "Using an oxygen-carrier as bed material for combustion of biomass in a 12-MWth circulating fluidized-bed boiler", *Fuel*, vol. 113, pp. 300–309, 2013, ISSN: 00162361. DOI: 10.1016/j.fuel.2013.05.073.

[9] M. Zevenhoven, P. Yrjas, B.-J. Skrifvars, and M. Hupa, "Characterization of Ash-Forming Matter in Various Solid Fuels by Selective Leaching and Its Implications for Fluidized-Bed Combustion", *ACS Publications*, vol. 26, no. 10, pp. 6366–6386, 2012. DOI: 10.1021/ef300621j. [Online]. Available: https://pubs.acs.org/sharingguidelines.

[10] M. Bartels, W. Lin, J. Nijenhuis, F. Kapteijn, and J. R. van Ommen, "Agglomeration in fluidized beds at high temperatures: Mechanisms, detection and prevention", *Progress in Energy and Combustion Science*, vol. 34, no. 5, pp. 633–666, 2008, ISSN: 0360-1285. DOI: https://doi.org/10.1016/j.pecs.2008.04.002. [Online]. Available: https://www.sciencedirect.com/science/article/pii/S0360128508000208.

[11] Britannica Academic. (2021). "Quartz", [Online]. Available: https://academic-eb-com.eu1.proxy.openathens.net/levels/collegiate/article/quartz/62182 (visited on 06/07/2021).

[12] Britannica Academic. (2021). "Silica mineral", [Online]. Available: https://academic-eb-com.eu1.proxy.openathens.net/levels/collegiate/article/silica-mineral/109688 (visited on 06/07/2021).

[13] Britannica Academic. (2021). "Silica", [Online]. Available: https://academic-eb-com.eu1.proxy.openathens.net/levels/collegiate/article/silica/67757 (visited on 06/07/2021).

[14] E. Brus, M. Öhman, A. Nordin, D. Boström, H. Hedman, and A. Eklund, "Bed agglomeration characteristics of biomass fuels using blast-furnace slag as bed material", *Energy & Fuels*, vol. 18, no. 4, pp. 1187–1193, 2004. DOI: 10.1021/ef034095c. eprint: https://doi.org/10.1021/ef034095c. [Online]. Available: https://doi.org/10.1021/ef034095c.

[15] B. Anicic, W. Lin, K. Dam-Johansen, and H. Wu, "Agglomeration mechanism in biomass fluidized bed combustion – reaction between potassium carbonate and silica sand", *Fuel Processing Technology*, vol. 173, pp. 182–190, 2018, ISSN: 0378-3820. DOI: https://doi.org/10.1016/j.fuproc.2017.10.005. [Online]. Available: https://www.sciencedirect.com/science/article/pii/S0378382017311700.

[16] C. Sevonius, P. Yrjas, and M. Hupa, "Defluidization of a quartz bed - Laboratory experiments with potassium salts", *Fuel*, vol. 127, pp. 161–168, 2014, ISSN: 00162361. DOI: 10.1016/j.fuel.2013.10.047.

[17] Jernkontoret. (Nov. 19, 2018). "Processes", [Online]. Available: https://www.jernkontoret.se/en/the-steel-industry/production-utilisation-recycling/processes/ (visited on 05/28/2021).

[18] Jernkontoret. (Nov. 19, 2018). "Slag, a very usable by-product", [Online]. Available: https://www.jernkontoret.se/en/the-steel-industry/production-utilisation-recycling/steel-production-residues/slag/ (visited on 02/24/2021).

[19] K. Davidsson, L.-E. Åmand, B.-M. Steenari, A.-L. Elled, D. Eskilsson, and B. Leckner, "Countermeasures against alkali-related problems during combustion of biomass in a circulating fluidized bed boiler", *Chemical Engineering Science*, vol. 63, no. 21, pp. 5314–5329, 2008, ISSN: 0009-2509. DOI: https://doi.org/10.1016/j.ces.2008.07.012. [Online]. Available: https://www.sciencedirect.com/science/article/pii/S000925090800362X.

[20] M. Rydén, M. Hanning, A. Corcoran, and F. Lind, "Oxygen Carrier Aided Combustion (OCAC) of Wood Chips in a Semi-Commercial Circulating Fluidized Bed Boiler Using Manganese Ore as Bed Material", *Applied Sciences*, vol. 6, no. 11, p. 347, 2016, ISSN: 2076-3417. DOI: 10.3390/app6110347. [Online]. Available: http://www.mdpi.com/2076-3417/6/11/347.

[21] F. Hildor, T. Mattisson, H. Leion, C. Linderholm, and M. Rydén, "Steel converter slag as an oxygen carrier in a 12 MWth CFB boiler – Ash interaction and material evolution", *International Journal of Greenhouse Gas Control*, vol. 88, pp. 321–331, 2019, ISSN: 17505836. DOI: 10.1016/j.ijggc.2019.06.019.

[22] H. Leion, T. Mattisson, and A. Lyngfelt, "Use of ores and industrial products as oxygen carriers in chemical-looping combustion", *Energy and Fuels*, vol. 23, no. 4, pp. 2307–2315, 2009, ISSN: 08870624. DOI: 10.1021/ef8008629.

[23] D. Yilmaz and H. Leion, "Interaction of Iron Oxygen Carriers and Alkaline Salts Present in Biomass-Derived Ash", 2020. DOI: 10.1021/acs.energyfuels.0c02109. [Online]. Available: https://dx.doi.org/10.1021/acs.energyfuels.0c02109.

[24] J. Udomsirichakorn and P. A. Salam, "Review of hydrogen-enriched gas production from steam gasification of biomass: The prospect of cao-based chemical looping gasification", *Renewable and Sustainable Energy Reviews*, vol. 30, pp. 565–579, 2014, ISSN: 1364-0321. DOI: https://doi.org/10.1016/j.rser.2013.10.013. [Online]. Available: https://www.sciencedirect.com/science/article/pii/S1364032113007120.

[25] Jernkontoret. (Nov. 19, 2018). "Steel production residues", [Online]. Available: https://www.jernkontoret.se/en/the-steel-industry/production-utilisation-recycling/steel-production-residues/ (visited on 02/24/2021).

[26] M. I. Martín, F. A. López, and J. M. Torralba, "Production of sponge iron powder by reduction of rolling mill scale", *Ironmaking & Steelmaking*, vol. 39, no. 3, pp. 155–162, 2012, ISSN: 0301-9233. DOI: 10.1179/1743281211Y.0000000078. [Online]. Available: http://www.tandfonline.com/doi/full/10.1179/1743281211Y.0000000078.

[27] P. Moldenhauer, M. Rydén, and A. Lyngfelt, "Testing of minerals and industrial by-products as oxygen carriers for chemical-looping combustion in a circulating fluidized-bed 300 W laboratory reactor", *Fuel*, vol. 93, pp. 351–363, 2012, ISSN: 00162361. DOI: 10.1016/j.fuel.2011.11.009.

[28] E. Jerndal, H. Leion, L. Axelsson, T. Ekvall, M. Hedberg, K. Johansson, M. Källén, R. Svensson, T. Mattisson, and A. Lyngfelt, "Utilisation de matériaux bon marché à base de fer comme transporteur d'oxygène dans la combustion en boucle chimique", *Oil and Gas Science and Technology*, vol. 66, no. 2, pp. 235–248, 2011, ISSN: 12944475. DOI: 10.2516/ogst/2010030. [Online]. Available: https://ogst.ifpenergiesnouvelles.fr/articles/ogst/abs/2011/02/ogst100062/ogst100062.html.

[29] H. Leion, E. Jerndal, B. M. Steenari, S. Hermansson, M. Israelsson, E. Jansson, M. Johnsson, R. Thunberg, A. Vadenbo, T. Mattisson, and A. Lyngfelt, "Solid fuels in chemical-looping combustion using oxide scale and unprocessed iron ore as oxygen carriers", *Fuel*, vol. 88, no. 10, pp. 1945–1954, 2009, ISSN: 00162361. DOI: 10.1016/j.fuel.2009.03.033.

[30] F. Störner, F. Hildor, H. Leion, M. Zevenhoven, L. Hupa, and M. R. Rydén, "Potassium Ash Interactions with Oxygen Carriers Steel Converter Slag and Iron Mill Scale in Chemical-Looping Combustion of Biomass Experimental Evaluation Using Model Compounds", 2020. DOI: 10.1021/acs.energyfuels.9b03616. [Online]. Available: https://dx.doi.org/10.1021/acs.energyfuels.9b03616.

[31] H. Leion, A. Lyngfelt, M. Johansson, E. Jerndal, and T. Mattisson, "The use of ilmenite as an oxygen carrier in chemical-looping combustion", *Chemical Engineering Research and Design*, vol. 86, no. 9, pp. 1017–1026, 2008, ISSN: 0263-8762. DOI: https://doi.org/10.1016/j.cherd.2008.03.019. [Online]. Available: https://www.sciencedirect.com/science/article/pii/S026387620800097X.

[32] A. Corcoran, J. Marinkovic, F. Lind, H. Thunman, P. Knutsson, and M. Seemann, "Ash properties of ilmenite used as bed material for combustion of biomass in a circulating fluidized bed boiler", *Energy & Fuels*, vol. 28, no. 12, pp. 7672–7679, 2014. DOI: 10.1021/ef501810u. eprint: https://doi.org/10.1021/ef501810u. [Online]. Available: https://doi.org/10.1021/ef501810u.

[33] F. Hildor, M. Zevenhoven, A. Brink, L. Hupa, and H. Leion, "Understanding the interaction of potassium salts with an ilmenite oxygen carrier under dry and wet conditions", *ACS Omega*, vol. 5, no. 36, pp. 22 966–22 977, 2020. DOI: 10.1021/acsomega.0c02538. eprint: https://doi.org/10.1021/acsomega.0c02538. [Online]. Available: https://doi.org/10.1021/acsomega.0c02538.

[34] C. Sevonius, "To be published", 2021.

[35] C. Sevonius, P. Yrjas, D. Lindberg, and L. Hupa, "Impact of sodium salts on agglomeration in a laboratory fluidized bed", *Fuel*, vol. 245, no. January 2018, pp. 305–315, 2019, ISSN: 00162361. DOI: 10.1016/j.fuel.2019.02.034.

[36] S. Hercules and D. M. Hercules. (Jul. 30, 2008). "Surface analysis", [Online]. Available: https://www.britannica.com/science/surface-analysis/Raman-spectroscopy#ref277287 (visited on 02/10/2021).

[37] S. Bradbury, D. C. Joy, and B. J. Ford. (May 3, 2010). “Scanning electron microscope, instrument”, [Online]. Available: https://www.britannica.com/technology/scanning-electron-microscope (visited on 02/10/2021).

[38] A. Nanakoudis. (Nov. 28, 2019). “Edx analysis with sem: How does it work?”, [Online]. Available: https://www.thermofisher.com/blog/microscopy/edx-analysis-with-sem-how-does-it-work/ (visited on 02/10/2021).

A

Appendix 1 - SEM-EDX images

A.1 Blast furnace slag

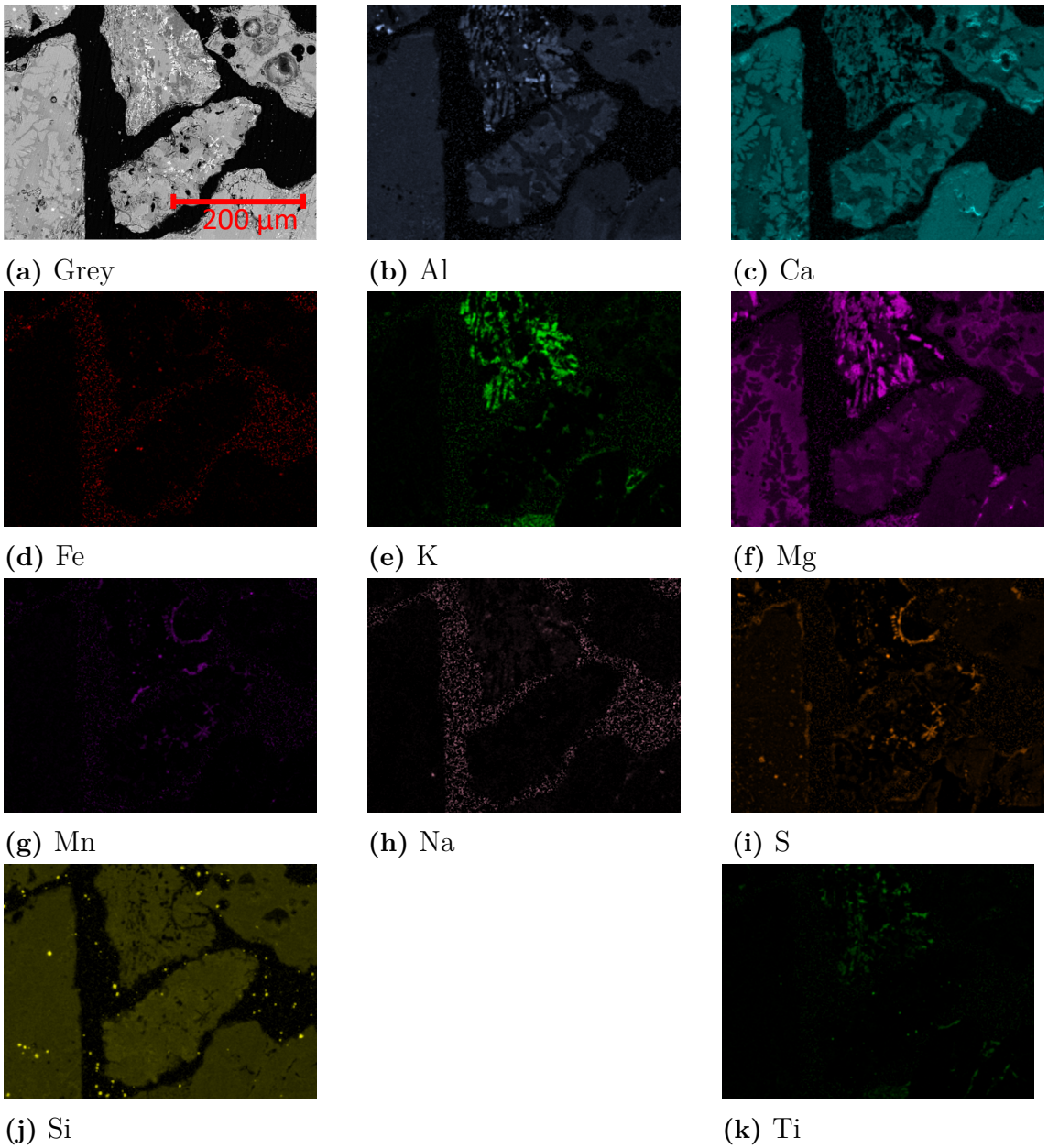

(a) Grey **(b)** Al **(c)** Ca

(d) Fe **(e)** K **(f)** Mg

(g) Mn **(h)** Na **(i)** S

(j) Si **(k)** Ti

Figure A.1: a) Backscattered SEM image of blast furnace slag before use in the reactor. b)-k) Representation of the elemental analysis as colored projections.

A.1.1 Blast furnace slag after sunflower seed shell pellets combustion

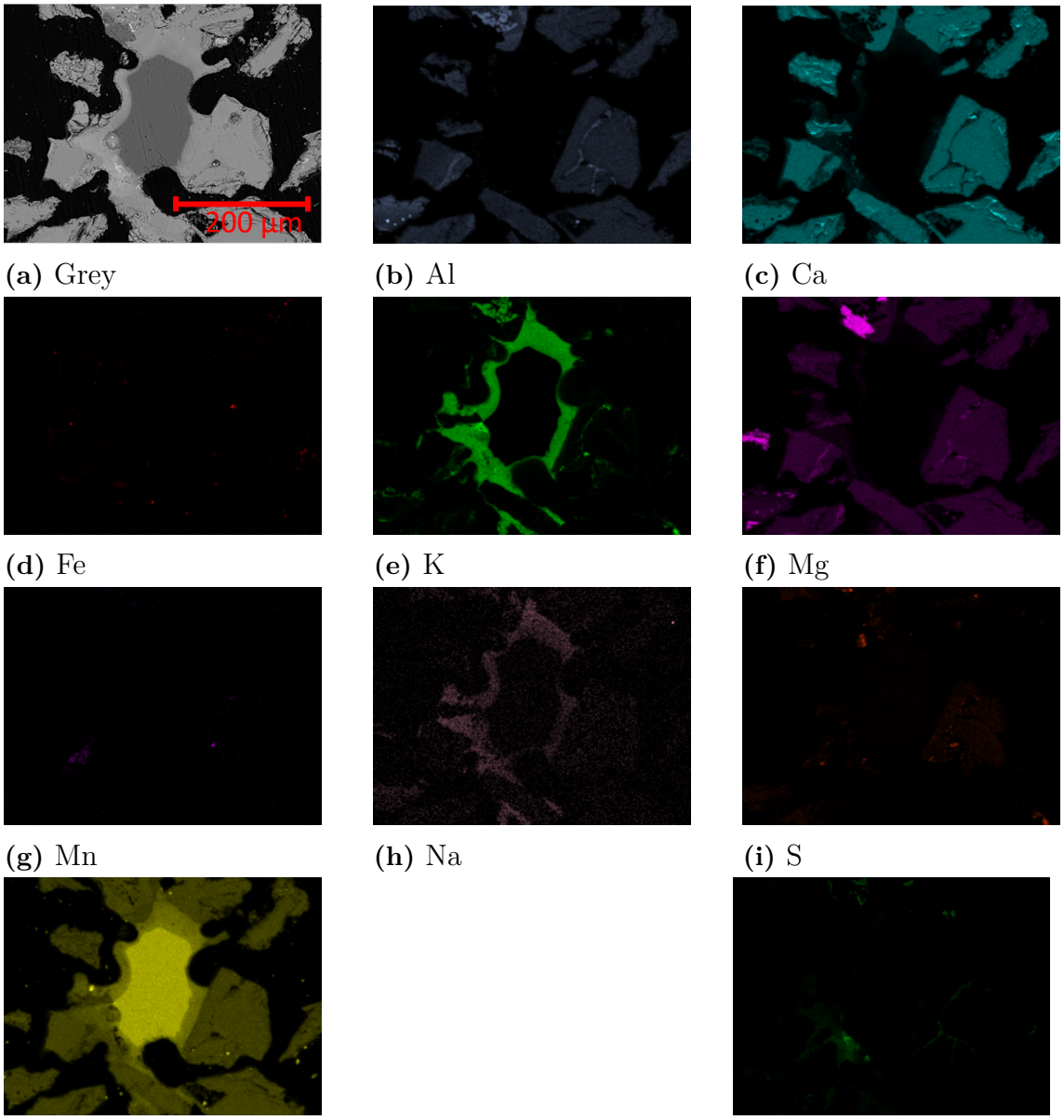

(a) Grey **(b)** Al **(c)** Ca

(d) Fe **(e)** K **(f)** Mg

(g) Mn **(h)** Na **(i)** S

(j) Si **(k)** Ti

Figure A.2: a) Backscattered SEM image of blast furnace slag after sunflower seed shell pellets combustion at 850°C. b)-k) Representation of the elemental analysis as colored projections.

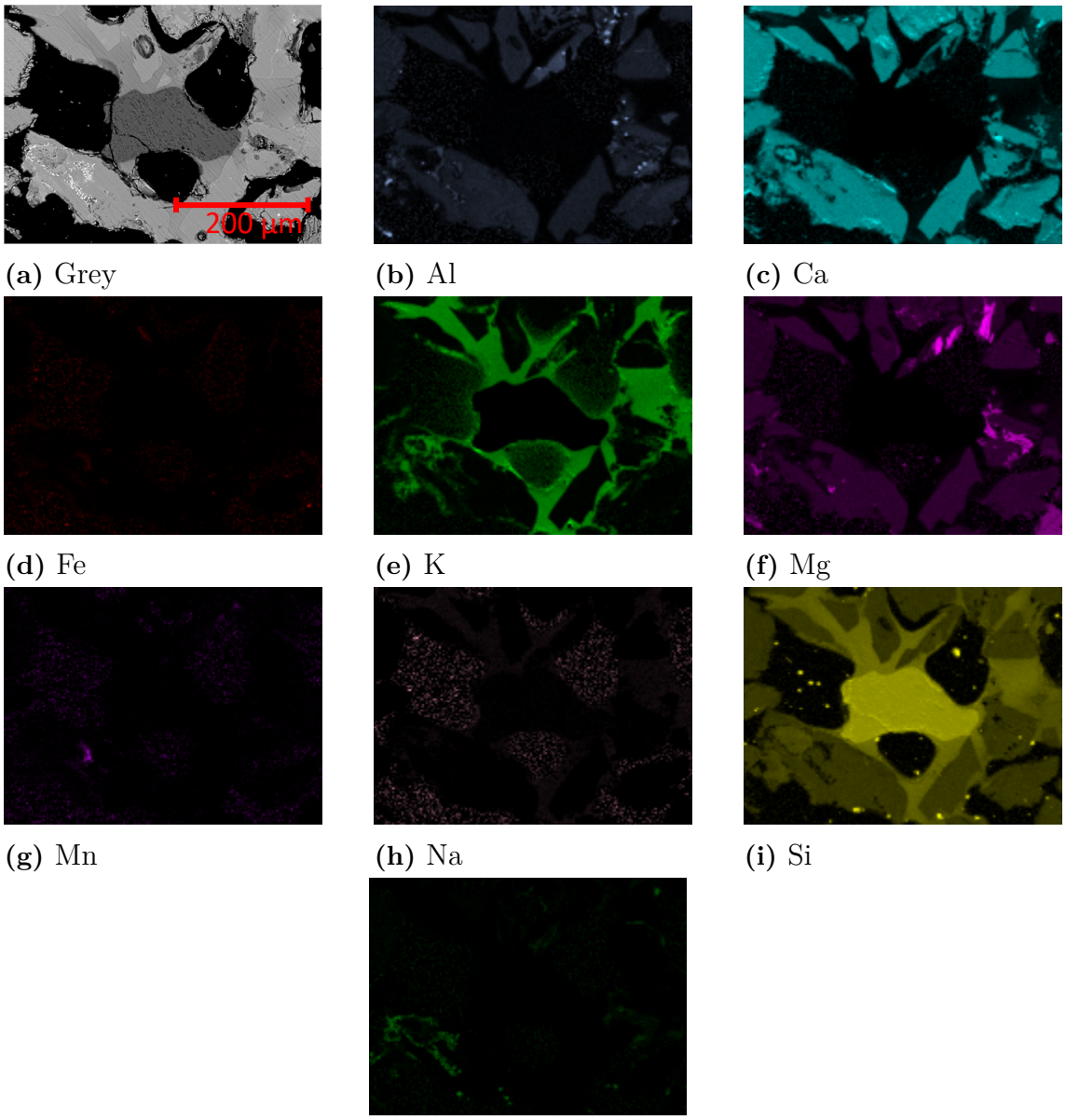

(a) Grey **(b)** Al **(c)** Ca

(d) Fe **(e)** K **(f)** Mg

(g) Mn **(h)** Na **(i)** Si

(j) Ti

Figure A.3: a) Backscattered SEM image of blast furnace slag after sunflower seed shell pellets combustion at 900°C. b)-j) Representation of the elemental analysis as colored projections.

A.1.2 Blast furnace slag after K_2CO_3 addition

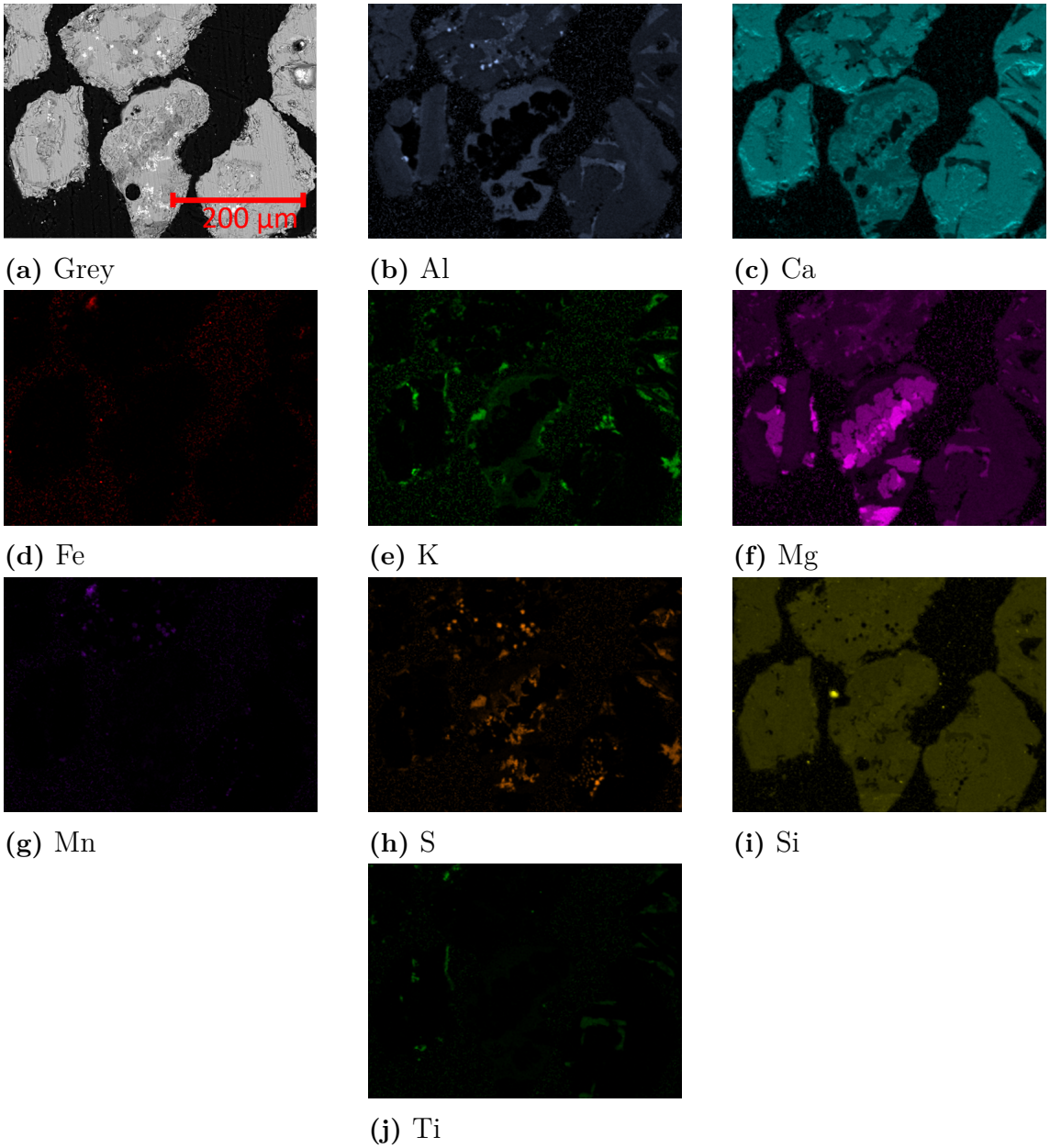

(a) Grey **(b)** Al **(c)** Ca

(d) Fe **(e)** K **(f)** Mg

(g) Mn **(h)** S **(i)** Si

(j) Ti

Figure A.4: a) Backscattered SEM image of blast furnace slag after K_2CO_3 addition at 850°C. b)-j) Representation of the elemental analysis as colored projections.

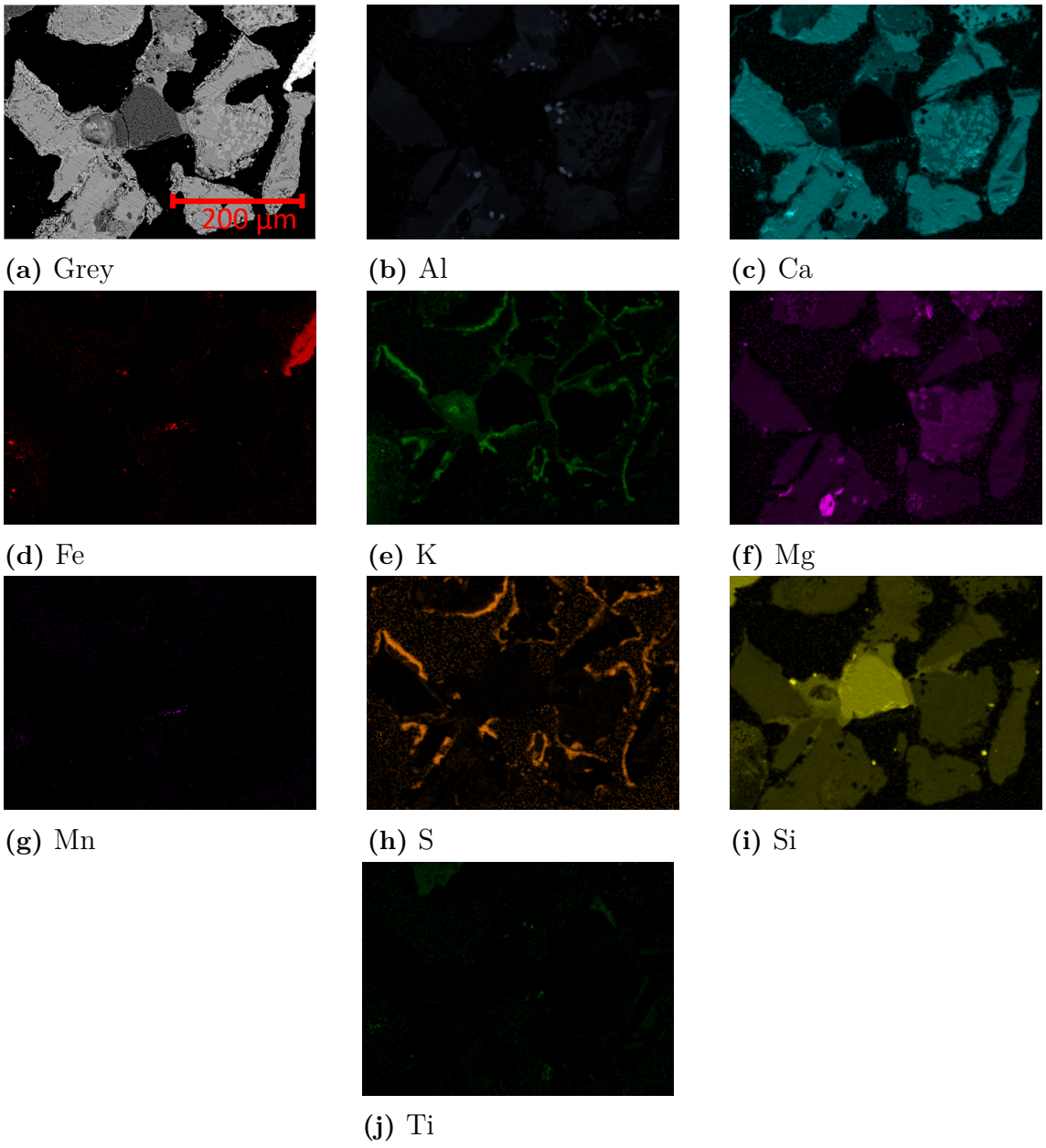

(a) Grey **(b)** Al **(c)** Ca

(d) Fe **(e)** K **(f)** Mg

(g) Mn **(h)** S **(i)** Si

(j) Ti

Figure A.5: a) Backscattered SEM image of blast furnace slag after K_2CO_3 addition at 900°C. b)-j) Representation of the elemental analysis as colored projections.

A.2 Oxide scale

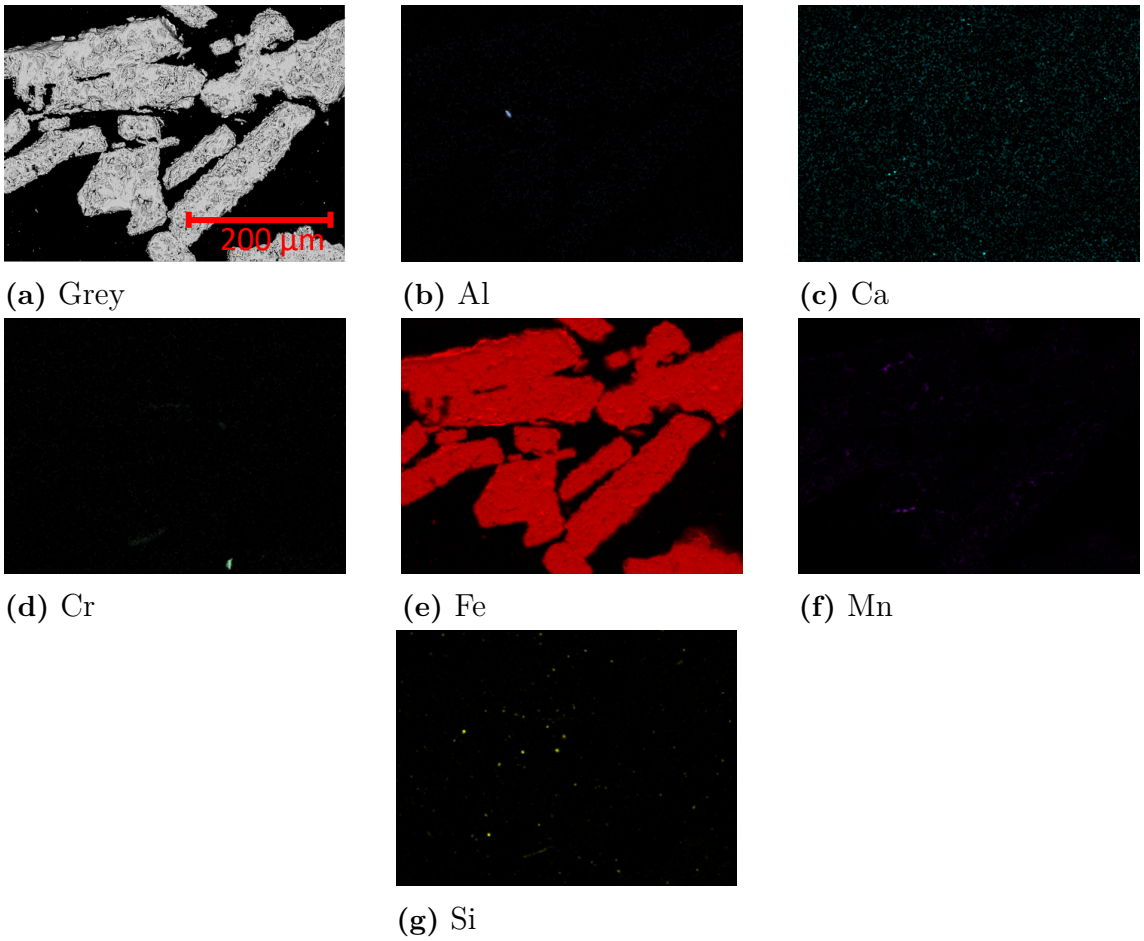

(a) Grey **(b)** Al **(c)** Ca

(d) Cr **(e)** Fe **(f)** Mn

(g) Si

Figure A.6: a) Backscattered SEM image of oxide scale before use in the reactor. b)-g) Representation of the elemental analysis as colored projections.

A.2.1 Oxide scale after sunflower seed shell pellets combustion

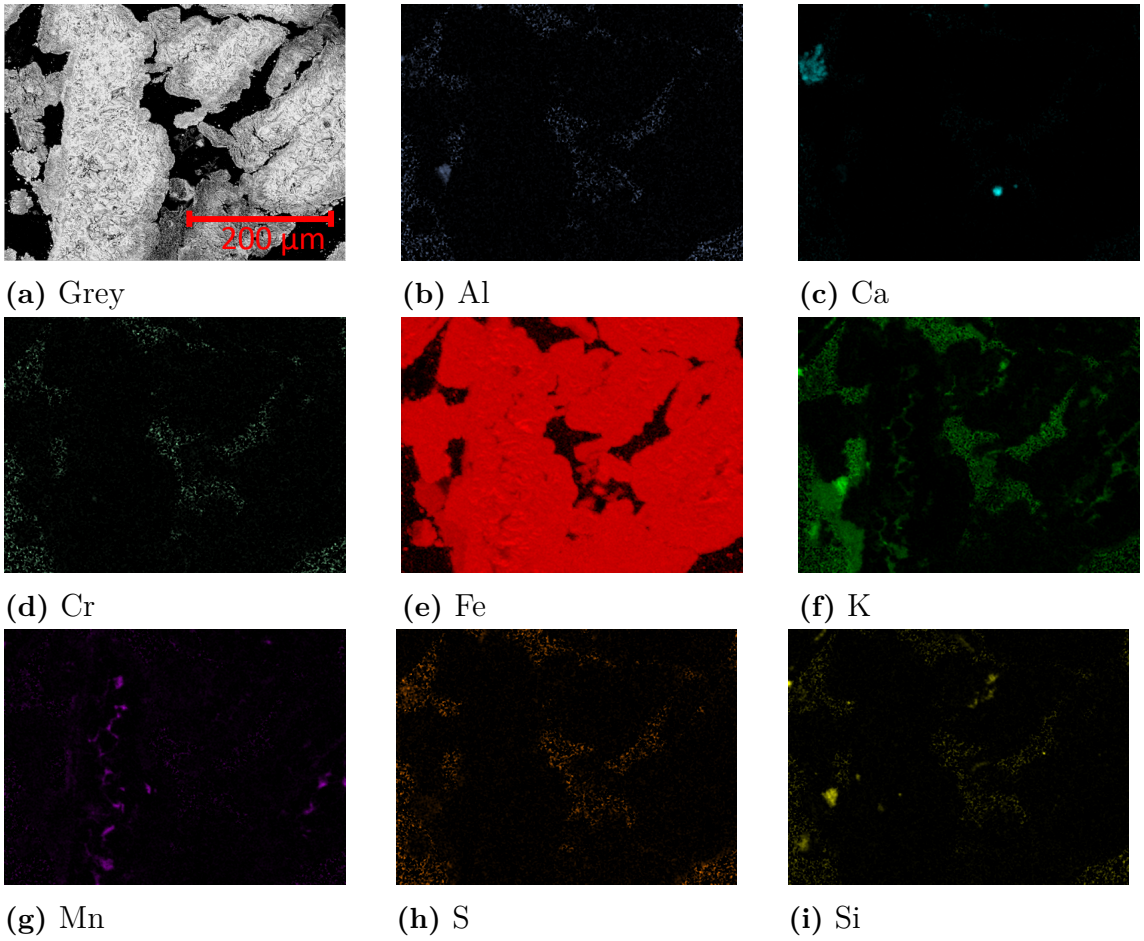

(a) Grey **(b)** Al **(c)** Ca

(d) Cr **(e)** Fe **(f)** K

(g) Mn **(h)** S **(i)** Si

Figure A.7: a) Backscattered SEM image of oxide scale after sunflower seed shell pellets combustion at 850°C. b)-i) Representation of the elemental analysis as colored projections.

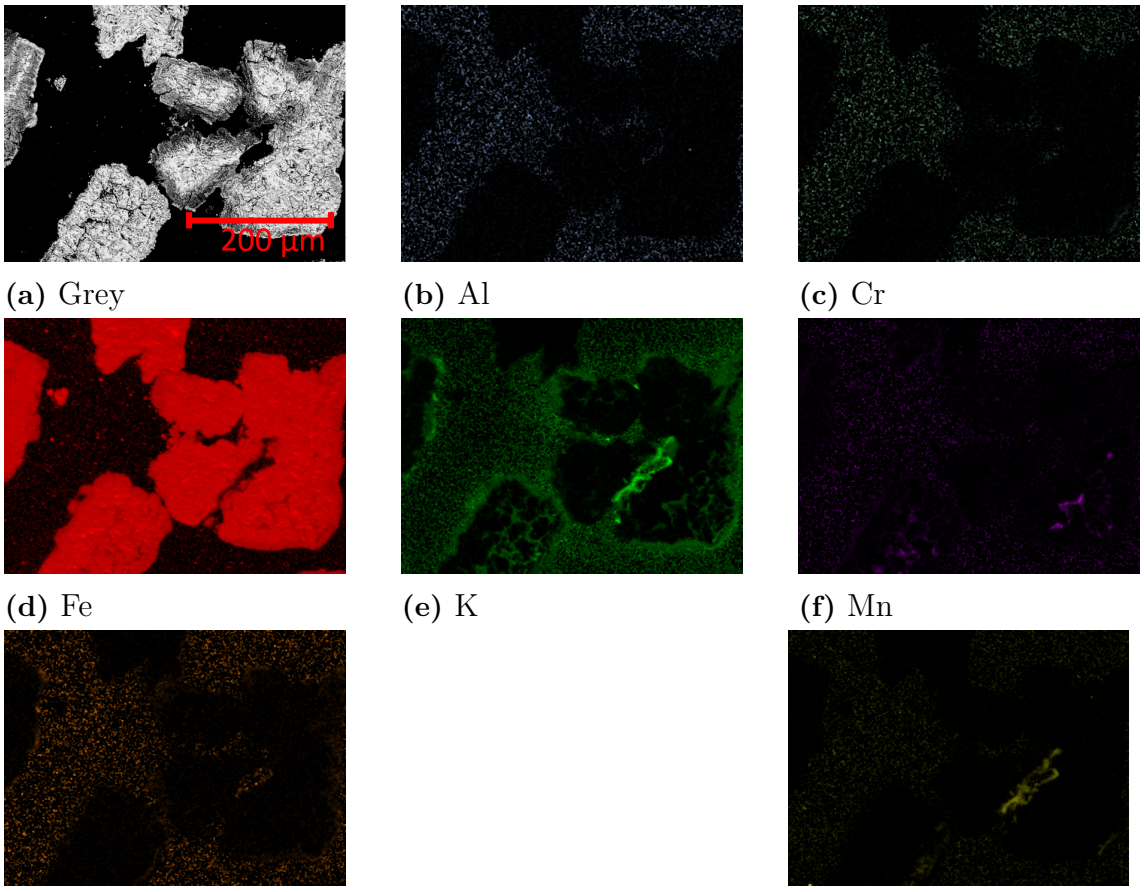

(a) Grey **(b)** Al **(c)** Cr

(d) Fe **(e)** K **(f)** Mn

(g) S **(h)** Si

Figure A.8: a) Backscattered SEM image of oxide scale after sunflower seed shell pellets combustion at 900°C. b)-h) Representation of the elemental analysis as colored projections.

A.2.2 Oxide scale after K_2CO_3 addition

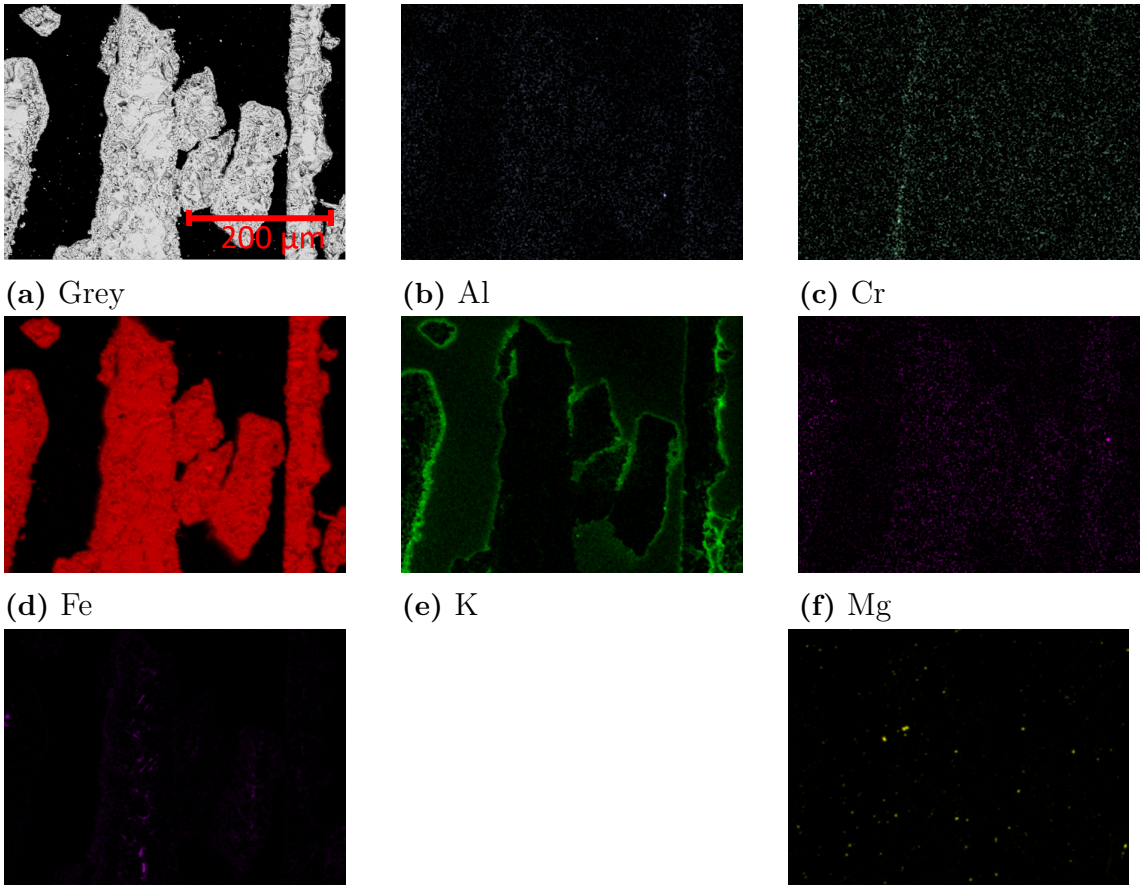

(a) Grey **(b)** Al **(c)** Cr

(d) Fe **(e)** K **(f)** Mg

(g) Mn **(h)** Si

Figure A.9: a) Backscattered SEM image of oxide scale after K_2CO_3 addition at 850°C. b)-h) Representation of the elemental analysis as colored projections.

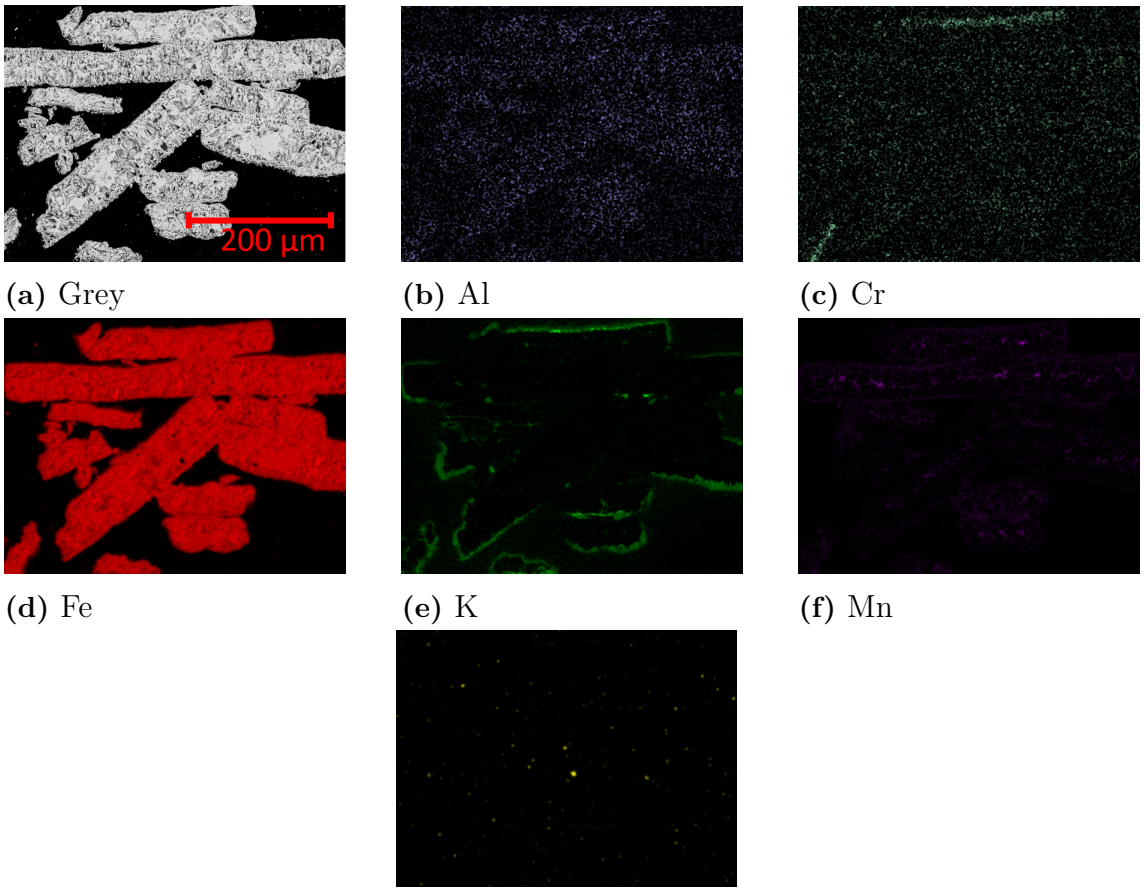

(a) Grey **(b)** Al **(c)** Cr

(d) Fe **(e)** K **(f)** Mn

(g) Si

Figure A.10: a) Backscattered SEM image of oxide scale after K_2CO_3 addition at 900°C. b)-g) Representation of the elemental analysis as colored projections.

B

Appendix 2 - Bed material composition

B.1 Blast furnace slag

Element	wt%
CaO	34.3
SiO	30.7
Al_2O_3	17.1
MgO	7.5
SO_3	3.2
Fe_2O_3	2.9
MnO_2	1.2
TiO	1.2
K_2O	1.2
Na_2O	0.7

Table B.1: Blast furnace slag composition in oxides.

B.2 Oxide scale

Element	wt%
Fe_2O_3	98.3
MnO_2	0.9
SiO_2	0.7

Table B.2: Oxide scale composition in oxides.

DEPARTMENT OF CHEMISTRY AND CHEMICAL ENGINEERING
CHALMERS UNIVERSITY OF TECHNOLOGY
Gothenburg, Sweden
www.chalmers.se

CHALMERS
UNIVERSITY OF TECHNOLOGY